Ecological Monographs, 90(1), 2020, e01399

Pulse of dissolved organic matter alters reciprocal carbon subsidies between autotrophs and bacteria in stream food webs

Benoît O. L. Demars,[1,2,5] Nikolai Friberg,[1,3,4] and Barry Thornton[2]

[1]*Norwegian Institute for Water Research (NIVA), Gaustaallen 21, Oslo 0349 Norway*
[2]*The James Hutton Institute, Craigiebuckler, Aberdeen AB15 8QH United Kingdom*
[3]*Freshwater Biological Section, University of Copenhagen, Universitetsparken 4, Third floor, Copenhagen 2100 Denmark*
[4]*School of Geography, University of Leeds, Leeds LS2 9JT United Kingdom*

Citation: Demars, B. O. L., N. Friberg, and B. Thornton. 2020. Pulse of dissolved organic matter alters reciprocal carbon subsidies between autotrophs and bacteria in stream food webs. Ecological Monographs 90(1):e01399. 10.1002/ecm.1399

Abstract. Soils are currently leaching out dissolved organic matter (DOM) at an increasing pace due to climate and land use change or recovery from acidification. The implications for stream biogeochemistry and food webs remain largely unknown, notably the metabolic balance (biotic CO_2 emissions) and carbon cycling between autotrophs and bacteria. We increased by 12% the flux of DOM in a stream for three weeks to mimic a pulse of natural DOM supply from soils rich in organic matter. We were able to track its fate into the food web through the use of a before and after control impact experimental design and the addition of DOM with a distinctive $\delta^{13}C$ signature. We used whole-stream metabolism to quantify carbon fluxes. Both photosynthesis and heterotrophic respiration increased rapidly following C addition, but this was short lived, likely due to nutrient limitations. Carbon exchange between autotrophs and bacteria in the control stream accounted for about 49% of bacterial production and 37% of net primary production, under stable flow conditions. Net primary production relied partly (19% in the control) on natural allochthonous dissolved organic carbon via the CO_2 produced by bacterial respiration, intermingling the green and brown webs. The preferential uptake of labile carbon by bacteria and excess bacterial CO_2 relative to nutrients (N, P) for autotrophs shifted the reciprocal carbon exchange between bacteria and autotrophs to a predominantly one-way carbon flow from bacteria to autotrophs, increasing the C:N:P molar ratios of autotrophs, the latter likely to become less palatable to consumers. The bacterial response to sucrose addition shifted the metabolic balance toward heterotrophy increasing biotic CO_2 emissions (+125%), shortened the average distance travelled by a molecule of organic matter (−40%), and thus provided less organic matter of lower quality for downstream ecosystems. Even a small increase in labile dissolved organic matter supply due to climate and land use change could significantly alter in-stream carbon cycling, with large effects on stream food web and biogeochemistry in small streams draining catchments with soils rich in organic carbon.

Key words: carbon cycle; dissolved organic matter; flow food web; microbial loop; nutrient spiraling; reciprocal subsidies; stoichiometry; whole-stream metabolism.

Introduction

The global annual riverine flux of organic C (0.26–0.53 Pg C/yr) to the oceans is comparable to the annual C sequestration in soil (0.4 Pg C/yr), suggesting that terrestrially derived aquatic losses of organic C may contribute to regulating changes in soil organic carbon storage (Dawson 2013). Soils are currently leaching out their organic matter at faster rates to aquatic ecosystems due to climate and land use change, or recovery from acidification (e.g., Freeman et al. 2004, Monteith et al. 2007, Drake et al. 2015). The fate of this organic matter in riverine systems remains poorly understood at the global scale, notably CO_2 emissions resulting from the mineralization of the organic matter (Drake et al. 2018). The role of terrestrial organic matter is also highly debated regarding its contribution to aquatic food webs (e.g., Cole 2013, Brett et al. 2017, Tanentzap et al. 2017, Drake et al. 2018). This may partly stem from an evolving understanding of the nature and structure of organic matter delivered to aquatic ecosystems.

The persistence (recalcitrance) of the organic matter in soils is more an ecosystem property than a characteristic of the molecular structure (aromaticity) of the organic matter (Schmidt et al. 2011, Dungait et al. 2012). The existence of humic macromolecules in soils has not been verified by direct measurements, suggesting the presence of simple biomolecules (Schmidt et al. 2011). Old carbon can also hold a large proportion of labile molecules such as sugars or acetate (Schmidt et al.

Manuscript received 7 October 2019; accepted 4 November 2019. Corresponding Editor: Stuart Findlay.
[5] E-mail: benoit.demars@niva.no

2011, Drake et al. 2015). The emerging understanding is that degradability of organic matter is more constrained by the biotic and abiotic environment (Schmidt et al. 2011, Dungait et al. 2012), such as C:N:P ecological stoichiometry (Evans et al. 2017, Kominoski et al. 2018), change in redox potential (e.g., Boye et al. 2017), and hydrological connectivity (e.g., Wilson et al. 2013, Marin-Spiotta et al. 2014, Demars 2019). This can explain the rapid turnover of allochthonous organic matter in aquatic ecosystems once it leaves the soil matrix (e.g., Marin-Spiotta et al. 2014, Drake et al. 2015, Demars 2019).

In streams, numerous dissolved organic matter (DOM) additions with simple compounds (from trace amount to 20 mg C/L) have repeatedly shown DOM use by bacteria and its transfer through the food chain (e.g., Warren et al. 1964, Hall 1995, Hall and Meyer 1998, Parkyn et al. 2005, Wilcox et al. 2005, Augspurger et al. 2008, Collins et al. 2016). Fewer studies used leaf leachate material (e.g., Cummins et al. 1972, Friberg and Winterbourn 1996, Wiegner et al. 2005, 2015), which are known to be processed at a slower rate than simple organic compounds (Mineau et al. 2016). Many studies have also traced the flux of autochthonous DOM through to bacteria (e.g., Neely and Wetzel 1995, Lyon and Ziegler 2009, Risse-Buhl et al. 2012, Kuehn et al. 2014, Hotchkiss and Hall 2015).

The potential benefit of bacterial CO_2 for primary producers has been hypothesized to explain a small increase (16–20%) in gross primary production following dissolved organic carbon addition and associated increase in bacterial activities (Robbins et al. 2017). This is a reasonable assumption (e.g., Redfield 1958, Butenschoen et al. 2016, Hasler et al. 2016) suggesting stream CO_2 limitation (at least within the boundary layer of photosynthesizing organisms and within biofilm, e.g., Hartley et al. 1996). Yet, the reciprocal carbon subsidies between autotrophs and bacteria in stream food webs have not been studied, to our knowledge, either empirically or theoretically. It raises the possibility that the carbon of the primary producers may be partly derived from allochthonous organic matter processed by the bacteria and intermingles the green and brown webs, similarly to the use of autotrophic DOM by bacteria.

The interactions between autotrophs and bacteria are, however, difficult to study (Amin et al. 2015), because primary producers, decomposers, and organic matter (allochthonous and autochthonous) are intricately connected both in benthic biofilms (Kamjunke et al. 2015, Battin et al. 2016) and pelagic aggregates (Grossart 2010). At the ecosystem scale, stream metabolism showed respiration to be generally tightly correlated to gross primary production across the globe, with respiration generally exceeding photosynthesis (Demars et al. 2016). Ecosystem respiration and primary production also tend to mirror each other throughout the year, although changes in canopy cover, hydrological events and pulses of allochthonous organic matter are known to affect this reciprocity (e.g., Uehlinger 2006, Bernhardt et al. 2018, Ulseth et al. 2018).

The extent to which an increase in CO_2 availability from bacterial respiration can boost primary production may be constrained by nutrient (N, P) availability (Fig. 1). Since natural DOM is generally poor in nutrients (Stutter et al. 2013) relative to bacterial tissue (Cotner et al. 2010), bacteria may shift from being nutrient regenerators to nutrient retainers (Cotner et al. 2010). Excess of CO_2 availability relative to N and P is expected to increase the C:N and C:P of autotrophs in nutrient-poor freshwater ecosystems (Hessen et al. 2004), possibly limiting their growth rate (Kahlert 1998, Hillebrand and Sommer 1999) and eventually reduce autotrophic C subsidies to bacteria. When respiration and photosynthesis are in synchrony, nutrient cycling rate increases with metabolic activity (Huryn et al. 2014), this is when bacteria depend strongly on autotrophic C and act as regenerators of N and P. Whether this holds during periods of asynchrony remains uncertain due to changes in net retention by autotrophs and heterotrophs (Roberts and Mulholland 2007).

Here we test how a small addition of labile organic carbon (sucrose, $C_{12}H_{22}O_{11}$) affects the strength and dynamics of the autotroph–bacteria reciprocal carbon

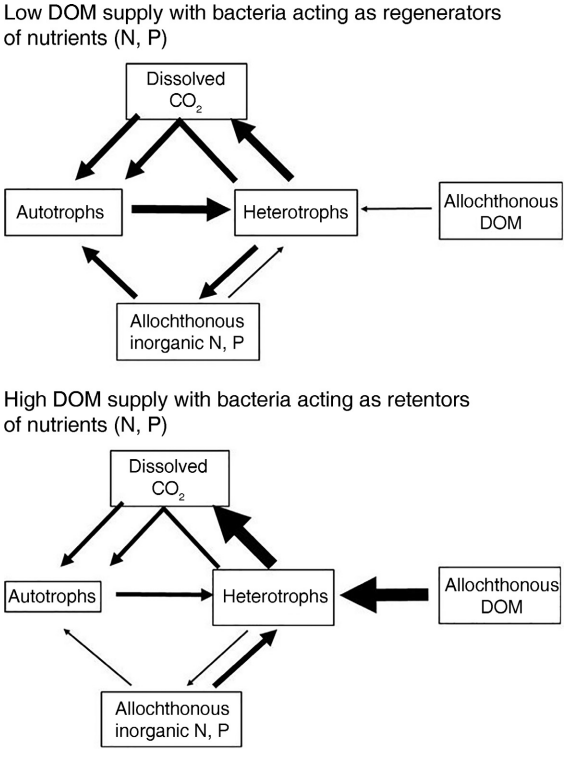

FIG. 1. Reciprocal carbon subsidies between autotrophs and bacteria in nutrient-poor stream food webs under contrasting supply of soil derived dissolved organic matter (allochthonous DOM). Arrows depict transfer of matter between the parts of the ecosystem. The size of the arrows is proportional to a priori hypotheses.

subsidies in phosphorus-poor streams draining soils rich in organic carbon. The time scale of the experiment (three weeks) corresponded to a pulse of soil derived DOM during a period of hydrological connectivity (wet soils) known to drive stream heterotrophic respiration in the studied streams (Demars 2019). We expected sucrose addition to (1) weaken reciprocal carbon exchanges between autotrophs and bacteria (Fig. 1); (2) shift the metabolic balance toward heterotrophy and thus increase biotic CO_2 emissions; (3) increase C : nutrient ratios in autotrophs and alter whole ecosystem nutrient (N, P) cycling rates; (4) reduce the organic carbon uptake length and speed up organic carbon uptake velocity; (5) reduce light use efficiency by primary production; and (6) increase organic carbon use efficiency by bacteria.

More fundamentally, we show how the overlooked carbon reciprocal transfers in streams affect food web ecology and biogeochemistry in the face of environmental changes.

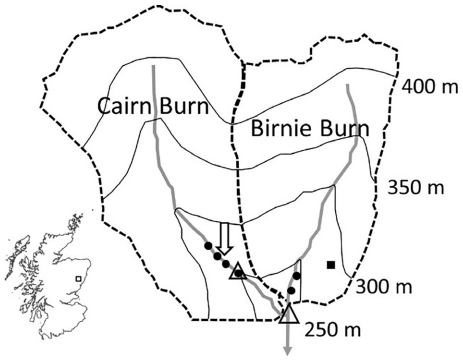

FIG. 2. Paired stream experiment at Glensaugh research station. Birnie Burn is the control stream and Cairn Burn the manipulated stream with DOM addition indicated by the arrow. The Cairn Burn also has a control upstream of the treatment reach. The symbols refer to flumes (open triangles), dissolved oxygen stations (solid circles), and soil moisture instrumentation (solid squares). The 50-m elevation contour lines are indicated. The catchment area is 0.99 km^2 (0.90 km^2 at the flume) for Cairn Burn and 0.76 km^2 for Birnie Burn. Inset shows the location of Glensaugh in Scotland.

METHODS

Strategy

The core of the study is based on a flow food web approach (sensu Marcarelli et al. 2011) and a whole-ecosystem before-after-control-impact (BACI) experimental design, adding sucrose with a distinctive $\delta^{13}C$ signature. We first present the study area and the nutrient (C, N, P) context. Second, we show how the food web was derived from whole-stream metabolism and carbon source apportionment (food web links). Third, we quantify C fluxes: calculations of whole-ecosystem CO_2 emissions (net ecosystem production, autotrophic and heterotrophic respiration), whole-stream production (net primary production and bacterial production), carbon and energy supplies (sucrose, natural allochthonous DOM, photosynthetic active radiation) and whole-ecosystem carbon cycling.

Study area

We studied two heather moorland catchments with soils rich in organic carbon, within the Glensaugh research station of the James Hutton Institute in north-east Scotland (2°33′ W, 57°55′ N; Fig. 2). Soil water, groundwater, and stream water have very low soluble reactive phosphorus concentrations (5 μg P/L; Demars 2019) independently of discharge variability. The streams were about 0.8–1.0 m wide in the studied sections and their channels significantly undercut the banks by 30–46% of stream width. Brown trout (*Salmo trutta fario*, Salmonidae) was present in both streams. The management of the land includes regular heather burning (10–12% of surface area yearly target) for hill farming: mixed grazing of sheep and cattle. For further information see Demars (2019).

The control stream

The control stream (Birnie Burn) is part of the long-term monitoring of the UK Environmental Change Network (ECN, data *available online*).[6] There is monitoring of soil temperature and moisture on the hillslope of the Birnie Burn at 275 m elevation (Cooper et al. 2007). Volumetric soil moisture content is recorded every 30 minutes at 10 and 45 cm depth, corresponding respectively to the base of the O (organic layer) and B (subsoil) horizons of the humus iron podzol present. The stream is equipped with a flume for continuous monitoring of discharge (catchment area 0.76 km^2) and dip water samples are collected weekly. This stream showed substantial increase in annual flow-weighted mean concentrations of stream-water dissolved organic carbon (DOC, +0.28 mg $C \cdot L^{-1} \cdot yr^{-1}$ during 1994–2007; Stutter et al. 2011). Water samples were analysed for DOC, pH, nutrients (N, P), and major ions. See Cooper et al. (2007), Stutter et al. (2012), and Demars (2019) for further details.

The paired stream

The control stream was paired with a neighboring stream (Cairn Burn) in 2005, also part of a long-term monitoring scheme with samples collected every week or two for stream water quality. In the late 1970s and early 1980s, two areas covering 33 ha were improved (reseeded, limed, and fertilized) as part of sheep grazing experiments (Hill Farming Research Organisation 1983). The added facilities at the Cairn Burn (catchment area 0.9 km^2) included a calibrated flume, water level, water

[6] http://data.ecn.ac.uk/.

electric conductivity, water and air temperature, and barometric pressure. Data were recorded every 5 minutes (CR10× data logger; Campbell Scientific, Logan, Utah, USA). Data logger, battery, and barometric pressure were housed in a weather-resistant enclosure. Photosynthetic active radiations (PAR) were also recorded in air, 1 m above ground, at the same time intervals (LICOR, Lincoln, Nebraska, USA). For more information, see Demars (2019).

Terrestrial DOM: main source of organic carbon

DOM was the dominant flux of organic carbon (98%) under stable flows with average concentrations of 9.3 ± 1.7 mg C/L in the two studied streams (Demars 2019). This DOM was of terrestrial origin as shown by $\delta^{13}C$ analyses of the natural DOM against terrestrial and aquatic plant material (Stutter et al. 2013). The median molar C:N:P stoichiometry of the DOM was 3201:103:1, with values ranging between 978:38:1 to 12,013:282:1 (Stutter et al. 2013). Chlorophyll *a* concentration in the water column was extremely low (<1 μg/L; Stutter et al. 2013). The pool of particulate organic carbon in the sediment is very small (Demars 2019), and coarse particulate organic carbon was less than 10 g C/m^2.

DOM addition

A carboy was refilled every 2 d with 6 kg of sucrose (granulated pure cane sugar, Tate & Lyle PLC, London, UK) dissolved in over 60 L of stream water filtered through muslin square in a large funnel. The carboy was set as a Mariotte bottle to ensure a constant dripping rate of 22 mL/minute lasting 48 h (15 mg C/s). The ventilation tube was netted at the top to avoid insect contamination. The dripping rate was kept constant over the 22 d of sucrose addition (23 August–14 September 2007) and was initially set to increase stream DOC concentration by about 0.5 mg C/L at 30 L/s. Samples were collected in washed bottles and filtered on site with prewashed filters (0.45-μm Millipore PVDF membrane filter; MilliporeSigma Filtration, now part of Merck, Darmstadt, Germany). DOC was determined within 48 h of collection with a Skalar San++ continuous flow analyzer (Breda, The Netherland), using potassium hydrogen phthalate as standards and sodium benzoate for quality controls. The detection limit was 0.1 mg C/L.

Nutrient cycling studies

Nutrient cycling studies were run in the control and manipulated streams before and during sucrose addition to test whether the expected increase in nutrient demand may be satisfied by faster cycling rate of N and P (hypothesis 3). Nutrient cycling rates were derived from continuous in situ nutrient addition experiments where a conservative tracer is also included (Stream Solute Workshop 1990, Demars 2008). This method tends to overestimate the nutrient uptake length S_w, average distance travelled by a nutrient molecule in the water column before river bed uptake. This is due to the addition of nutrient compared to isotopic tracer studies (e.g., Mulholland et al. 2002). However, preliminary tests in the Cairn Burn showed that the bias can be kept small (10–15%) with small nutrient additions (Demars 2008). Nitrate (as KNO_3) and phosphate (as KH_2PO_4) were continuously added together with NaCl as conservative tracer (cf Schade et al. 2011). The target molar stoichiometric ratio for the addition was N:P ≈ 20, similar to the periphyton optimal ratio for growth (Hillebrand and Sommer 1999) but differential uptake of N and P in the mixing zone led to slightly higher average added molar N:P ratios (34 and 70 in the control and treatment reach, respectively). This was similar to the average background molar ratio of the treatment reach at the time of the nutrient additions (N:P = 58), but somewhat lower than the control (N:P = 206). When the plateau phase was reached, water samples were collected at about 10-m intervals along the reach and filtered on site (pre-washed 0.45 μm Millipore PVDF membrane filter; see Demars 2008). The samples were kept cool at 4–10°C. The nutrients (PO_4 and NO_3) were determined within 48 h by colorimetry using a Skalar San++ continuous flow analyzer (Breda, The Netherland) and chloride by ion chromatography (Dionex DX600, Sunnyvale, California, USA). The limits of detections were 0.001 for NO_3 and PO_4 and 0.003 mg/L for Cl. In order to provide a more comparable indicator of nutrient cycling for different hydrological conditions, the uptake velocity v_f was also calculated as follows: $v_f = (u \times z)/S_w$, with u being average water velocity and z average depth. Short uptake lengths and fast uptake velocities indicate fast cycling rates (high exchange rates between water and benthos).

Flow food web

We determined whole-stream metabolism to test the effect of DOM addition on net ecosystem production (NEP, corresponding to biotic CO_2 emissions; hypothesis 2). This approach also gives gross primary production (GPP) and ecosystem respiration (ER) from which net primary production (NPP) and heterotrophic production (HP) can be derived knowing the carbon use efficiency and bacterial growth efficiency, respectively. This, combined with a knowledge of C source apportionment, allows to build the flow food web from which the C reciprocal subsidy hypothesis between autotrophs and bacteria can be tested.

Whole-stream metabolism

Whole-stream metabolism was estimated by the open channel two-station diel oxygen method of Odum (1956) modified by Demars et al. 2011, 2015, 2017 and

Demars (2019). Many tracer studies (using NaCl and propane) were carried out as detailed in Demars et al. (2011) to estimate lateral inflows, mean travel time, and reaeration coefficient as a function of discharge within the range of stable flows (up to 32 L/s). The relationships with discharge in our three stream reaches were very strong (Appendix S1: Fig. S1, Demars 2019) allowing accurate parameterization of metabolism calculations under varying flow conditions, similarly to previous studies (e.g., Roberts et al. 2007, Beaulieu et al. 2013). The high oxygen reaeration coefficient of those streams (0.05–0.24 per minute) required very accurate dissolved O_2 data. Oxygen concentrations were measured with optic sensors fitted on multiparameter sondes TROLL9500 Professional (In-Situ Inc., Fort Collins, Colorado, USA) and Universal Controller Sc100 (Hach Lange GMBF, Düsseldorf, Germany), the latter powered with two 12-V DC (75 mA) car batteries per sensor kept charged with two 20 W solar panels (SP20 Campbell Scientific). The sensors were calibrated to within 1% dissolved oxygen saturation. Four sondes were deployed in the Cairn Burn at 0, 84, 138, and 212 m upstream of the flume to include an extra control reach (138–212 m) upstream of the manipulated reach (0–84 m). Another two sondes were set in the control stream Birnie Burn at an 88-m interval (60–148 m upstream of the ECN flume). The distances between oxygen stations corresponded to 80–90% of the oxygen sensor footprints ($3u/k_2$), with u/k_2 entirely independent of discharge ($R^2 = 0.0005$), which allowed the manipulated reach to be independent of the control reach. The DOM injection point was 28 m upstream of the top station of the manipulated reach, and this distance corresponded to 69% of the oxygen sensor footprint of the top station. All sondes were deployed from May to October 2007, logging at 5-minute intervals.

The net metabolism was only calculated for stable flow conditions (3–32 L/s), as follows (Demars 2019):

$$\mathrm{NEP}_t = \left(\frac{C_{\mathrm{AV}t+\Delta t} - C_{\mathrm{AV}t}}{\Delta t} - k_2(C_s - C_{\mathrm{AV}t}) - \frac{\theta(C_g - C_{\mathrm{AV}t})}{\Delta t}\right) z$$

with NEP_t, net ecosystem production at time t (g $O_2 \cdot m^{-2} \cdot minute^{-1}$); C_{AV}, average dissolved oxygen (g O_2/m^3) of the two stations at time $t + \Delta t$ and t (minutes); Δt, time interval (minutes); k_2, oxygen exchange coefficient (per minute); C_s, saturated oxygen concentration (g O_2/m^3); θ, the proportion of lateral inflows (Q_g/Q); z, average stream depth (m); and C_g, oxygen concentration in lateral inflows (g O_2/m^3). The latter was calculated as follows (from base flow analysis of stream hydrographs):

$$C_g = (1/(1 + \exp(a \ln(Q) - b))0.9C_s) + (1 - 1/(1 + \exp(a \ln(Q) - b))0.1C_s)$$

with Q, discharge; and a and b, constants; permitting to correct for base flow (first term of the equation) and soil water (second term of the equation) lateral inflows; see Demars (2019). The proportion (mean ± SE) of total lateral inflows relative to discharge (Q_g/Q) was 10.7% ± 0.6%, 6.6% ± 0.5%, and 2.3% ± 0.4% for the Birnie Burn control, Cairn Burn control, and treated reach, respectively, independently of discharge in the range 3.8–32.5 L/s (stable flows).

All calculations were run in Excel (Microsoft, Redmond, Washington, USA) using a preformatted spreadsheet (Demars 2019). The overall uncertainties in daily stream metabolism, including cross-calibration errors, individual parameter uncertainties, spatial heterogeneity (through the average of diel O_2 curves), and correction for lateral inflows, were propagated through all the calculations using Monte Carlo simulations (Demars 2019). The corrections for lateral inflows amounted to about 6% of ER for the treated reach (Cairn Burn), 19% and 16% in the control reaches, Cairn Burn and Birnie Burn, respectively.

Identification of carbon sources and pathways

Macrophytes.—The percentage cover of bryophytes and filamentous green algae was measured with a ruler across transects taken every 2 m along the stream reaches. Young shoots of filamentous green algae and bryophytes were collected by hand along both studied reaches before and after sucrose addition. All samples were freeze dried and milled prior to analyses for C, N, $\delta^{13}C$, and $\delta^{15}N$. The main source of inorganic carbon for primary producers was assumed to be CO_2 because of the low alkalinity (remaining below 0.5 meq HCO_3/L under low flows). The fractionation factor for CO_2 assimilation into macrophyte tissue is known to vary with pCO_2 and growth rate, and was set at −25.5‰ ± 3.5‰ within the range of Rubisco forms IA and IB in the absence of carbon concentrating mechanism and transport limitation (22–29‰, e.g.; Raven et al. 1994, McNevin et al. 2007, Boller et al. 2015). Net primary production was assumed to be driven by filamentous green algae and biofilm autotrophs. Bryophytes were not used to calculate the flow food webs.

Inorganic carbon.—The $\delta^{13}C$ of dissolved CO_2 was estimated indirectly under low flows using the fractionation factor of Rubisco −25.5‰ ± 3.5‰ and $\delta^{13}C$ of bryophytes (strict CO_2 user and no CO_2 transport limitation). In our study, the average $\delta^{13}C$ of bryophytes was −36.4‰, and assuming the above fractionation coefficient of −25.5‰, Glensaugh $\delta^{13}C$ of dissolved CO_2 would be −10.9‰. This is similar to the $\delta^{13}C$ of DIC (6–14‰ under low flows; Waldron et al. 2007) and $\delta^{13}C$ of bryophytes (−33.3‰; Palmer et al. 2001) reported for the Brocky Burn (a stream running on the other side of the hill). The proof of concept comes from another Scottish stream (Dighty Burn), where Raven et al. (1994) reported the $\delta^{13}C$ of dissolved CO_2 as −14.7‰ and bryophytes as −39.2‰, suggesting a fractionation

coefficient of −24.5‰ by difference. In our calculations under low flow conditions, we therefore assumed $\delta^{13}C$ of dissolved CO_2 as −11‰ ± 3‰.

To quantify the reciprocal subsidies between autotrophs and bacteria, it remained to partition the overall stable isotope signature of stream dissolved CO_2 into the allochthonous (groundwater, soil water and atmospheric exchange) and autochthonous (respiration by heterotrophs and autotrophs) sources. The allochthonous signature, $\delta^{13}C_{CO2\text{-allochthonous}}$, can be deduced from rearranging the following three-ended mixing model:

$$F_{CO2} \times \delta^{13}C_{CO2} = F_{CO2-\text{allochthonous}} \times \delta^{13}C_{CO2-\text{allochthonous}} + F_{CO2-\text{heterotrophs}} \times \delta^{13}C_{CO2-\text{heterotrophs}} + F_{CO2-\text{autotrophs}} \times \delta^{13}C_{CO2-\text{autotrophs}}$$

where F_{CO2} represents CO_2 fluxes (g C·m^{-2}·d^{-1}, with all fluxes expressed as positive values) and $\delta^{13}C$ the isotope signature (‰) of the different sources of CO_2. We averaged the $\delta^{13}C$ of the autotrophs (filamentous green algae and biofilm primary producers). The $\delta^{13}C_{CO2\text{-allochthonous}}$ was only calculated for the control stream under low stable flows and assumed to apply to both streams. Uncertainties were propagated in quadrature using standard deviation δx for sums, and relative uncertainties $\delta x/x$ for the division.

Sucrose.—The $\delta^{13}C$ of sucrose from sugar cane is similar to that of dissolved CO_2 (−12‰ ± 1‰; Jahren et al. 2006, Augspurger et al. 2008, Kankaala et al. 2010, de Castro et al. 2016), but sucrose uptake by autotrophs was assumed to be without isotopic discrimination (Wright and Hobbie 1966). The proportion of carbon derived from added sucrose (F_S) in organic matter, primary producers and bacteria was calculated from their $\delta^{13}C$ in the control (C) and treatment (T) reaches, before (subscript B) and after (subscript A) sucrose addition as follows:

$$F_s = \frac{T_A - (T_B + (C_A - C_B))}{-12 - (T_B + (C_A - C_B))}$$

with all uncertainties propagated in quadrature using standard deviation δx for sums, and relative uncertainties $\delta x/x$ for the division. The standard error of the mean was calculated as SEM = $\delta x/\sqrt{n}$ with n average number of samples in C_B, C_A, T_B, T_A.

Allochthonous organic carbon.—The $\delta^{13}C$ of the DOM (mean ± SD) was available from a previous study from the same catchment and showed it was of terrestrial origin, i.e., not autochthonous ($\delta^{13}C$ = −28.5‰ ± 0.3‰; Stutter et al. 2013). Coarse particulate organic matter (CPOM) was also collected by hand along both studied reaches before and after sucrose addition. Since there was hardly any difference in $\delta^{13}C$ between DOM and CPOM ($\delta^{13}C$ = −27.4‰ ± 0.7‰, Appendix S1: Table S1), we used the $\delta^{13}C$ of CPOM determined in this study as the signature for allochthonous organic carbon.

Periphyton.—Periphyton (or biofilm) samples represent a mixture of primary producers (algae and cyanobacteria), bacteria and fine particulate organic matter. The samples were collected before and at the end of the sucrose addition from the flumes and stones with a toothbrush, funnel, and bottle. All samples were freeze-dried and milled.

We also placed six pairs (with/without petroleum jelly) of unglazed ceramic tiles (10 × 10 cm) fixed on bricks and deployed along the studied reaches in both streams three weeks before the start of the manipulation. Vaseline was applied around half the tiles to prevent grazing by invertebrates. After three weeks, there was hardly any growth on the tiles, and so the tiles were left in the stream until thze end of the manipulation. One brick in the control stream was lost. At the end of the experiment, the tiles were frozen at −20°C, later freeze-dried, and the biofilm was scraped with a razor blade. Since there was little biomass per tile (about 1 g C/m^2), the biofilm was pooled by stream and grazer treatments (leaving two samples per stream). Very little grazing activity was observed on the tiles during the six weeks and unsurprisingly no difference in biofilm dry mass emerged due to grazer exclusion (paired t tests on ln-transformed mass; Birnie, t_4, $P = 0.13$; Cairn, t_5, $P = 0.26$).

Phospholipid fatty acids (PLFAs) were extracted from the biofilm samples from the tiles and derivatized to their methyl esters (FAMES) following the procedure of Frostegård et al. (1993) using the modified extraction method of Bligh and Dyer (1959), as detailed in Certini et al. (2004). Quantification and $\delta^{13}C$ values of the PLFAs were both determined by Gas Chromatography-Combustion-Isotope Ratio Mass Spectrometry (GC-C-IRMS) as described by Main et al. (2015), and averaged for each stream ($\delta^{13}C$, Appendix S1: Table S2). Only PLFAs up to 19 carbon chain length were determined (excluding some long-chain essential polyunsaturated fatty acids, e.g., Muller-Navarra et al. 2000, Gladyshev et al. 2011).

Bacterial carbon.—The bacterial PLFAs were identified as those most affected by sucrose addition in the treated reach and information derived from the literature (Appendix S1: Table S2). This also allowed us to determine the $\delta^{13}C$ of bacteria in the control reach. We assumed a fractionation factor of −3‰ for the $\delta^{13}C$ of bacterial fatty acids relative to bulk tissue samples (Hayes 2001). This is within the range of observed values in other studies (Boschker and Middelburg 2002, Bec et al. 2011). We used the same fractionation factor of −25.5‰ ± 3.5‰ for the assimilation of CO_2 coming

from bacterial respiration into green algal tissue. Since we only had comparative data for the treatment period, the fraction of sucrose within PLFAs was calculated as follows:

$$F_s = \frac{T_A - C_A}{-12 - 3 - C_A}.$$

Biofilm autotroph carbon.—The carbon from cyanobacteria and algae was identified from a specific PLFA (α-linolenic acid, Risse-Buhl et al. 2012) using the same fractionation factor as above between PLFA and bulk tissue (Appendix S1: Table S2), knowing that this fractionation factor can vary between individual PLFAs and taxonomic groups (Taipale et al. 2015).

Analytical methods.—The total carbon and total nitrogen concentrations and the $\delta^{13}C$ and $\delta^{15}N$ natural abundance isotope ratios of the milled samples were determined using a Flash EA 1112 Series Elemental Analyzer connected via a Conflo III to a Delta^{Plus} XP isotope ratio mass spectrometer (all Thermo Finnigan, Bremen, Germany). The isotope ratios were traceable to reference materials USGS40 and USGS41 (both L-glutamic acid); certified for $\delta^{13}C$ (‰ VPDB) and $\delta^{15}N$ (‰ air N_2). The carbon and nitrogen contents of the samples were calculated from the area output of the mass spectrometer calibrated against National Institute of Standards and Technology standard reference material 1547 peach leaves, which was analyzed with every batch of 10 samples. Long-term accuracies for a quality control standard (milled flour) were as follows: total carbon, 40.3% ± 0.35%; $\delta^{13}C$, −25.4% ± 0.13‰; total nitrogen, 1.7% ± 0.04%; and $\delta^{15}N$, 1.90% ± 0.26‰ (mean ± SD, n = 200). Data processing was performed using Isodat NT software version 2.0 (Thermo Electron, Bremen, Germany) and exported into Excel. Total P was determined after a 30-minute digestion in 50% nitric acid at 120°C (see Demars and Edwards 2007) for CPOM, bryophytes, biofilm, and green filamentous algae in order to test for expected changes in C:N:P stoichiometry (hypothesis 3).

Data analyses for carbon sources and pathways.—Most studies use $\delta^{13}C$ and $\delta^{15}N$ to identify the flow path in the food web. Here the BACI experimental design allowed us to calculate the proportion of sucrose (*Fs*) in all parts of the food web. *F*s was used as a tracer in addition to $\delta^{13}C$ to determine the sources of carbon for bacteria and algae in the treatment reach after 22 d of sucrose addition. Thus, the carbon pathways were identified with carbon tracers. While F_s in the sources was determined from the change in $\delta^{13}C$ due to sucrose addition, the sources had different initial $\delta^{13}C$ and different coefficients of isotopic discrimination (or TEF, trophic enrichment factor), and this decoupled F_s from $\delta^{13}C$ as shown in the isospace plots (Appendix S1: Figs. S2 and S3). End-member mixing analyses were used to determine the proportion of C sources and their uncertainties in primary producers and bacteria. We provided the numerical solutions given by a Bayesian stable isotope mixing model using MixSIAR 3.1.9 (Parnell et al. 2010, 2013, Stock and Semmens 2016) in R version 3.5.0 (R Core Team 2018). We checked that the mixture data were within the range of the sources (see raw data in Appendix S1: Table S3 and S4 and illustrations in Appendix S1: Figs. S2 and S3). The numerical solutions converged rapidly according to the Markov chain Monte Carlo convergence diagnostics (Gelman-Rubin and Geweke). The numerical solutions of MixSIAR were also very similar to the analytical solutions of IsoError 1.04 (Phillips and Gregg 2001) and suggested that the results were not biased (cf Brett 2014).

Quantification of carbon fluxes

To assess trophic transfer efficiencies in the food web, our production estimates were all standardized to g C·m^{-2}·d^{-1}. Respiration and photosynthesis rates in oxygen were converted to carbon using a respiratory and photosynthetic quotient of 1 (Williams and del Giorgio 2005, but see Berggren et al. 2012). Total CO_2 emissions (F_{CO2}) were estimated to derive $\delta^{13}C_{CO2\text{-allochthonous}}$ in the three-ended mixing model presented above and to estimate the relative proportion of biotic CO_2 emissions. In order to calculate carbon and light use efficiencies of the food webs (hypotheses 5 and 6), we determined net biotic productions and fluxes of carbon and energy supplies (sucrose, natural allochthonous DOM, photosynthetic active radiation). Finally, we could derive carbon uptake length and uptake velocity from heterotrophic production and DOM supply (hypothesis 4).

Total CO_2 emissions.—In the absence of direct measurements, the excess partial pressure of CO_2 (EpCO$_2$) of the streams was estimated from three measured parameters: pH, alkalinity and temperature (Neal et al. 1998; as applied in Demars et al. [2016] with atmospheric CO_2 = 384 ppm, data *available online*).[7] Our EpCO$_2$ estimates had high uncertainties (±50%; Demars 2019). EpCO$_2$ is the concentration of free CO_2 in the stream water (C_t at time t) relative to the atmospheric equilibrium free CO_2 concentration (C_{SAT}):

$$Ep\mathrm{CO}_2 = C_t / C_{\mathrm{SAT}}.$$

C_{SAT} was calculated from published CO_2 solubility in pure water at equilibrium with atmospheric CO_2 in the temperature range 0°–90°C (Carroll et al. 1991) and Henry's law (Stumm and Morgan 1981, Butler 1982). C_t was calculated as EpCO$_2$ × C_{SAT}. The flux of CO_2 (F_{CO_2}, g C m^{-2} d^{-1}) at the interface between water and

[7] ftp://ftp.cmdl.noaa.gov/ccg/co2/trends/co2_annmean_mlo.txt

the atmosphere was calculated as for O_2 following Young and Huryn (1998):

$$F_{CO_2} = k_{CO_2}(C_{SAT} - C_t)\tau\frac{Q}{A}$$

with k_{CO_2}, reaeration coefficient of CO_2 (per d); C_{SAT} and C_t (mg C/L or g C/m^3); τ, mean travel time of the stream reach (d); Q, average water discharge (m^3/d); and A, surface water area of the stream reach (m^2). The reaeration coefficients between CO_2 and O_2 can be simply related as follows (Demars et al. 2015, Demars 2019):

$$k_{CO_2} = \frac{Dm_{CO_2}}{Dm_{O_2}}k_{O_2} = 0.81 \pm 0.01\, k_{O_2}$$

based on the molecular diffusivity (D_m) of CO_2 and O_2 measured at three different temperatures within the same study (Davidson and Cullen 1957), assuming dissolved gas solubility played a negligible role in the studied streams with little gas exchange area due to air bubbles (cf Hall and Madinger 2018).

The flux of CO_2 was then related to discharge within the range of low stable flows for which stream metabolism was processed (Cairn $n = 47$, $R^2 = 0.81$; Birnie $n = 65$, $R^2 = 0.77$) to provide daily estimates. For more details, see Demars (2019).

Biotic CO_2 emissions.—These were simply calculated as the net ecosystem production (NEP), gross primary production (GPP) plus ecosystem respiration (ER, a negative flux) expressed in g C·m^{-2}·d^{-1}. Bacterial respiration of DOM was calculated as heterotrophic respiration (HR, a negative flux) from

$$HR = ER + \alpha GPP \text{ with } \alpha = AR/GPP$$

with AR, autotrophic respiration, and ER, ecosystem respiration, both negative fluxes (oxygen consumption) and GPP, positive flux (producing oxygen). We partitioned ER into auto and heterotrophic respiration with α = 0.5 (see Demars et al. 2015) and calculated uncertainties using α = 0.2 and α = 0.8. Bacterial respiration of the added sucrose was calculated as the difference in heterotrophic respiration between the treatment and a control reach during sucrose addition, after standardizing for site differences using the control period.

Whole-stream production.—We calculated net ecosystem primary production (NPP) by assuming a 50% carbon use efficiency (ε = 1 − α), that is one-half GPP (reviewed in Demars et al. 2015, 2017) and computed NPP for ε = 0.2 and ε = 0.8 to provide uncertainties in our estimates. Heterotrophic production (HP, g C·m^{-2}·d^{-1}) was calculated from heterotrophic growth efficiency HGE and heterotrophic respiration (HR, negative flux expressed in g C·m^{-2}·d^{-1}) as follows:

$$HP = \frac{-HR \times HGE}{1 - HGE}.$$

Heterotrophic production was estimated for low (5%) and moderate (20%) bacterial growth efficiencies (e.g., Berggren et al. 2009, Fasching et al. 2014, Berggren and del Giorgio 2015).

Allochthonous organic matter.—The overall flux at the outlet of both streams was calculated as discharge times DOC concentration using the weekly data from the long-term ECN monitoring collected in 2007–2008 under low stable flows. The DOC flux was then related to discharge (Cairn $n = 74$, $R^2 = 0.85$; Birnie $n = 100$, $R^2 = 0.83$), to provide an estimate for the days for which DOC was not measured (within the same range of flows).

The organic carbon uptake length ($S_{w\text{-}OC}$, in m) and mineralization velocity ($v_{f\text{-}OC}$, in m per d) were calculated as in previous studies (Newbold et al. 1982, Hall et al. 2016), here neglecting POC (see above):

$$Sw_{OC} = \frac{Q \times [DOC]}{-HR \times w}$$

with [DOC], dissolved organic carbon concentration (g C·m^{-3}·d^{-1}); Q, discharge (m^3); HR, heterotrophic respiration (a negative flux expressed in g C·m^{-2}·d^{-1}); w, width (m); and

$$v_{f-OC} = \frac{-HR}{[DOC]}.$$

Light.—We derived a conversion factor for photosynthetically active radiation (PAR; 1 mol photon·m^{-2}·d^{-1} = 6.13 g C·m^{-2}·d^{-1}) by relating the ratio of total quanta to total energy within the PAR spectrum (2.5×10^{21} photon·s^{-1}·kJ^{-1} = 4.15×10^{-3} mol photon/kJ; Morel and Smith 1974) with the reciprocal of the energy content of glucose expressed in carbon units (15.7 kJ/g glucose = 25.4×10^{-3} g C/kJ; Southgate and Durnin 1970).

Sucrose.—The flux of added sucrose over the treatment reach was determined at the top of the reach (84 m upstream of the flume of Cairn Burn) using the average observed increase in DOC concentrations (28 August, 5 September, 11 September 2007) multiplied by discharge (Appendix S1: Fig. S4).

Ecosystem efficiencies

With all fluxes expressed in g $C \cdot m^{-2} \cdot d^{-1}$, we calculated the light use efficiency (net primary production/photosynthetic radiations), organic carbon use efficiency (bacterial production/DOC supply), and the proportion of biotic CO_2 emissions (net ecosystem production/total CO_2 emissions).

Data analyses of the experiment (stream reach scale)

We calculated an effect size (i.e., proportional changes) of sucrose addition on our response variables (e.g., nutrient cycling, stoichiometric ratios, metabolic fluxes, ecosystem efficiencies) using the values of the control (C) and treatment (T) reaches, before (subscript B) and after (subscript A) sucrose addition as follows:

$$\text{Effect size} = ((C_B - C_A) - (T_B - T_A))/T_B$$

with all uncertainties propagated in quadrature using standard deviation δx for sums, and relative uncertainties $\delta x/x$ for the division. Since the overall design was unreplicated, we simply reported the effect size in relation to the relative uncertainties or one standard deviation (equivalent to 68% confidence interval of our measurement errors). We did not calculate a standard error of the mean because our samples were pseudo-replicated (random collection was within one plot) or temporally autocorrelated (daily stream metabolism; see Hurlbert 1984). We therefore did not report P values. The interpretation of the results will be based on the strength of the effect size, knowledge from previous experiments addressing individual aspects of our study, and hypothetical standard errors based on varying the number of replicated studies.

The control period for the metabolic parameters and trophic transfer efficiencies was limited to the 2 d prior to sucrose addition (21–22 August), so the whole data series was within a single period of stable flows, i.e., not interrupted by peak flows, producing more comparable results across sites.

Results

Experimental DOM addition

Stable flows were present during the whole three weeks of carbon addition (Fig. 3). The target concentration was achieved at the top of the studied reach, 28 m downstream of the injection point, where the DOM addition averaged 0.52 mg C/L above background concentration (Appendix S1: Fig. S4).

Stream metabolism continuous monitoring

Gross primary production (GPP) peaked to 7.6 g $O_2 \cdot m^{-2} \cdot d^{-1}$ 10–11 d after the start of sucrose addition in the treatment reach before decreasing sharply down to an average 2.4 g $O_2 \cdot m^{-2} \cdot d^{-1}$ during the last 4 d of the carbon addition, and this despite high photosynthetic active radiations. In contrast, GPP remained relatively constant in the control reaches Birnie Burn (about 1.2 g $O_2 \cdot m^{-2} \cdot d^{-1}$) and Cairn Burn (3.2 g $O_2 \cdot m^{-2} \cdot d^{-1}$ for the first two weeks declining to 2.1 g $O_2 \cdot m^{-2} \cdot d^{-1}$ during the last week g $O_2 \cdot m^{-2} \cdot d^{-1}$; Fig. 3). Bryophytes covered 4, 11 and 17% of the river bed in the Birnie control, Cairn control and Cairn treatment reach, respectively. Filamentous green algae (mostly *Microspora* sp., Microsporaceae) percentage cover increased during the period of sucrose addition from 1% to 19%, 11% to 33%, and 4% to 37% of channel width in the Birnie control, Cairn control, and Cairn treatment reach, respectively.

Peaks in ecosystem respiration (ER) to −20 g $O_2 \cdot m^{-2} \cdot d^{-1}$ (Birnie Burn) and −35 g $O_2 \cdot m^{-2} \cdot d^{-1}$ (Cairn Burn) were more visible for the controls than the treatment reach, with respiration activity inversely related to soil hydrological connectivity, as recorded by soil moisture continuous monitoring (Fig. 3). There was an increase in ER in the treatment reach at the start of the sucrose addition, despite the continuing loss of hydrological connectivity. While ER mirrored GPP with a 4-d time lag ($ER_{t+4\ d} = -1.06 \pm 0.12 \times GPP_t - 4.23 \pm 0.64$ g $O_2 \cdot m^{-2} \cdot d^{-1}$; $R^2 = 0.79$), heterotrophic respiration activity associated to sucrose addition peaked sharply 15 d after the start of the addition, independently of GPP and autotrophic carbon use efficiency, processing up to 59% of the daily sucrose flux (Appendix S1: Fig. S5). On average 35% ± 20% of the added sucrose was respired during the addition over just 84 m (or 15 minutes mean travel time). Heterotrophic production ranged between 2% and 10% of the sucrose flux, based on bacterial growth efficiencies of 0.05 and 0.20, respectively.

Nutrient cycling studies and stoichiometry

The background concentrations of nitrate and phosphate were 180 and 90 μg N/L and 2 and 4 μg P/L in the Birnie control and Cairn treatment reach, respectively. The added geometric mean of N and P were on average 471 μg N/L and 24 μg P/L. The addition of sucrose had no effect on nitrate and phosphate nutrient uptake length and uptake velocity (Fig. 4, Appendix S1: Table S5). The phosphate uptake length was highly related to discharge and became very short, down to 31 m in the treatment reach toward the end of the sucrose addition. Phosphate uptake velocity was about 0.2 mm/s and an order of magnitude faster than nitrate with uptake lengths in the kilometer range.

The molar C:N:P stoichiometric ratios of coarse particulate organic matter and bryophytes remained stable throughout the experiment. Sucrose addition exerted strong effects on filamentous green algae and periphyton stoichiometry (Fig. 5, Appendix S1: Table S6). While the molar C:N:P stoichiometric ratios decreased in the

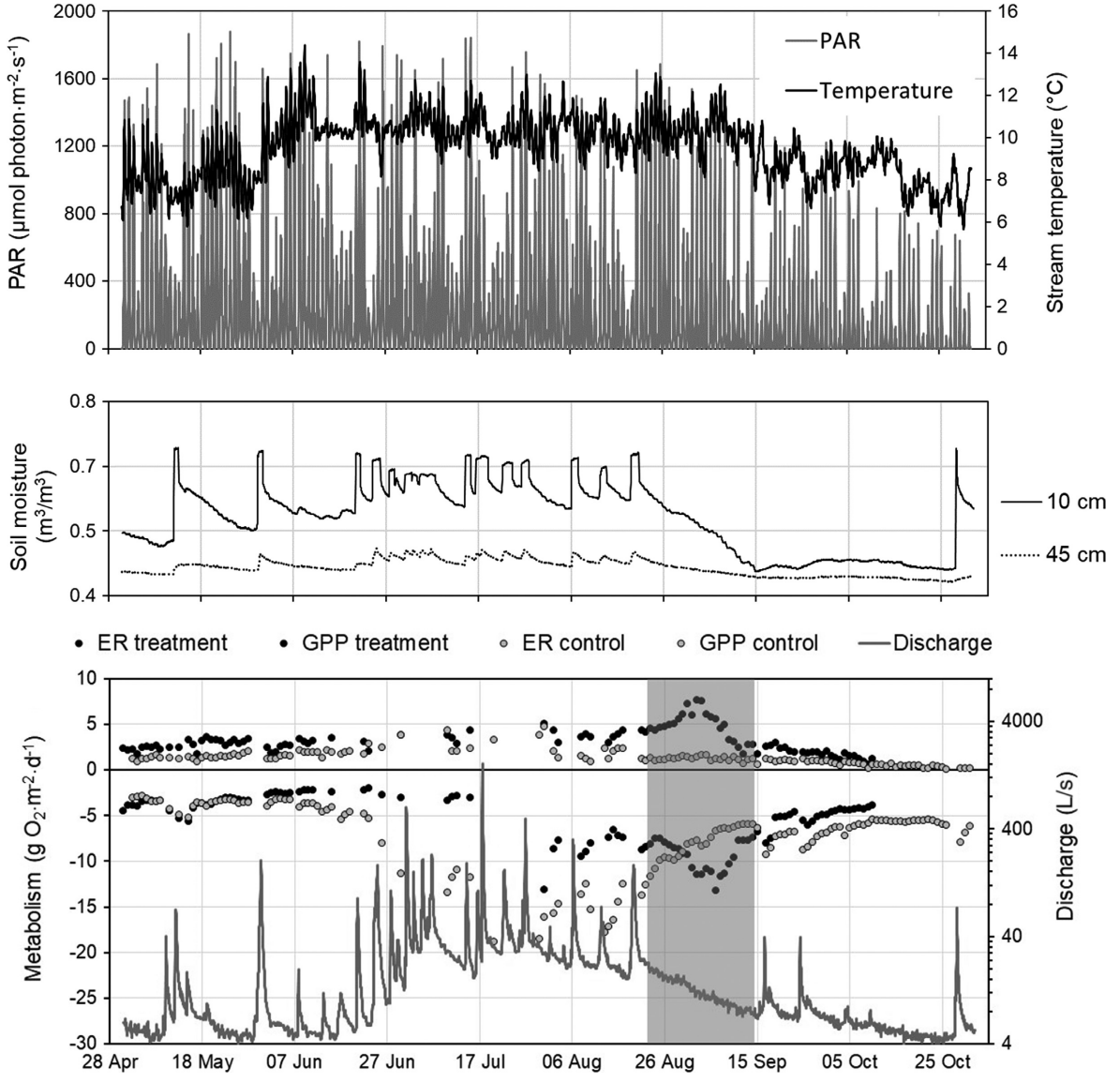

FIG. 3. Continuous data monitoring and stream metabolism in the control reach (Birnie Burn) and treatment reach (Cairn Burn). Ecosystem respiration (ER) is negative (consuming O_2) and gross primary production (GPP) is positive (producing O_2). The period of DOM (sucrose) addition (23 Aug–14 Sep) is indicated by gray shading. The depths for soil moisture correspond to the depths of the organic soil (10 cm) and subsoil (45 cm).

control stream, they increased sharply in the treatment reach following sucrose addition: from 330:29:1 to 632:49:1 in filamentous green algae and from 262:29:1 to 428:38:1 in periphyton.

Fate of added sucrose

In the treatment reach, the fraction of carbon derived from sucrose (F_S) was relatively high in filamentous green algae (24% ± 0.07%), biofilm autotrophs (algae and cyanobacteria, 36% ± 13%), and heterotrophs (bacteria 68% ± 14%), and absent from CPOM and bryophytes (Appendix S1: Fig. S6, Appendix S1: Table S1).

Identification of carbon sources and pathways under stable flows (end of experiment)

The autotrophs (filamentous green algae and periphyton autotrophs) derived 63% ± 14% of their CO_2 from allochthonous sources (groundwater and atmosphere) and 37% ± 14% from autochthonous bacteria in the control reach. In the treatment reach, autotrophs derived a similar proportion of CO_2 from allochthonous sources (61% ± 8%), some osmotrophic uptake of sucrose (13% ± 8%), and relatively less from bacteria (26% ± 11%). The bacteria used equally autotrophic carbon (49% ± 15%) and allochthonous organic carbon

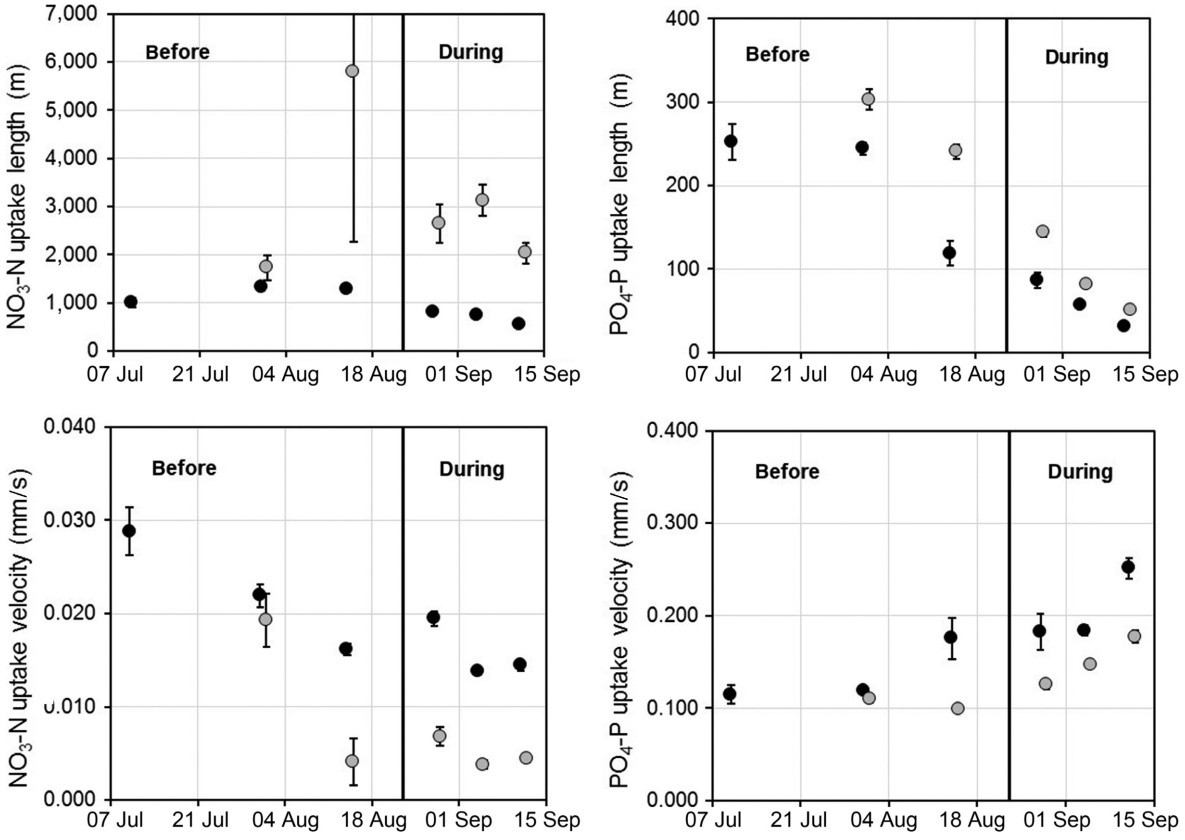

FIG. 4. Stream nutrient uptake length (S_w) and uptake velocity (v_f) before and during sucrose addition in the control (gray symbols) and treatment (black symbols). Error bars represent SE, with some error bars smaller than the symbols. Note the different magnitudes on the *y*-axes between NO_3-N and PO_4-P.

(51% ± 15%) in the control but used more added sucrose (62% ± 7%) than autotrophic (19% ± 11%) and natural allochthonous organic matter (18% ± 10%) in the treatment reach; see Fig. 6.

Quantification of biotic carbon fluxes

Our estimates suggest that in the control 0.07–0.34 g $C{\cdot}m^{-2}{\cdot}d^{-1}$ of net primary production (0.23 ± 0.14 g $C{\cdot}m^{-2}{\cdot}d^{-1}$) was used for bacterial production (0.15–0.69 g $C{\cdot}m^{-2}{\cdot}d^{-1}$), and in turn 0.09 ± 0.06 g $C{\cdot}m^{-2}{\cdot}d^{-1}$ of the CO_2 fixed by autotrophs was derived from bacterial CO_2, although it represented a small fraction of bacterial respiration (2.77 g $C{\cdot}m^{-2}{\cdot}d^{-1}$) driving net ecosystem production (biotic CO_2 emissions, 2.53 g $C{\cdot}m^{-2}{\cdot}d^{-1}$; see Fig. 7). In the treatment, during sucrose addition, net primary production (0.91 ± 0.55 g $C{\cdot}m^{-2}{\cdot}d^{-1}$) was higher than the control but bacterial production (0.14–0.66 g $C{\cdot}m^{-2}{\cdot}d^{-1}$) was similar. The flow of C was much higher from bacteria to autotrophs (0.24 ± 0.18 g $C{\cdot}m^{-2}{\cdot}d^{-1}$) than from autotrophs to bacteria (0.03–0.13 g $C{\cdot}m^{-2}{\cdot}d^{-1}$), sucrose being the major source of C for bacteria (0.09–0.41 g $C{\cdot}m^{-2}{\cdot}d^{-1}$). The estimated flux of natural allochthonous organic matter assimilated by bacteria was 66% higher in the control (0.08–0.35 g $C{\cdot}m^{-2}{\cdot}d^{-1}$) than in the treatment (0.03–0.12 g $C{\cdot}m^{-2}{\cdot}d^{-1}$), and still 41% higher after standardizing by the difference in natural DOC supply.

Ecosystem carbon fluxes

Photosynthetic active radiation (light) decreased slightly from 106 to 80 and 118 to 90 g $C{\cdot}m^{-2}{\cdot}d^{-1}$ in the control and treatment respectively. Total CO_2 emissions (range 10–29 g $C{\cdot}m^{-2}{\cdot}d^{-1}$) were higher before than during the treatment period, and higher in the control than in the treatment, reflecting differences in hydrological connectivity with soil water between sites and period of time. The flux of natural allochthonous organic matter (DOM) was more than halved from 177 to 85 and 110 to 50 g $C{\cdot}m^{-2}{\cdot}d^{-1}$ in the control and treatment due to the soils becoming dryer (Fig. 3). This was reflected by a general reduction in the organic carbon uptake length 3,214 to 2,531 m and 4,257 to 1,886 m in the control and treatment, respectively, independently of the carbon addition. The organic carbon uptake velocity decreased in the control from 0.82 to 0.55 m/d but increased in the treatment from 0.53 to 0.76 m/d.

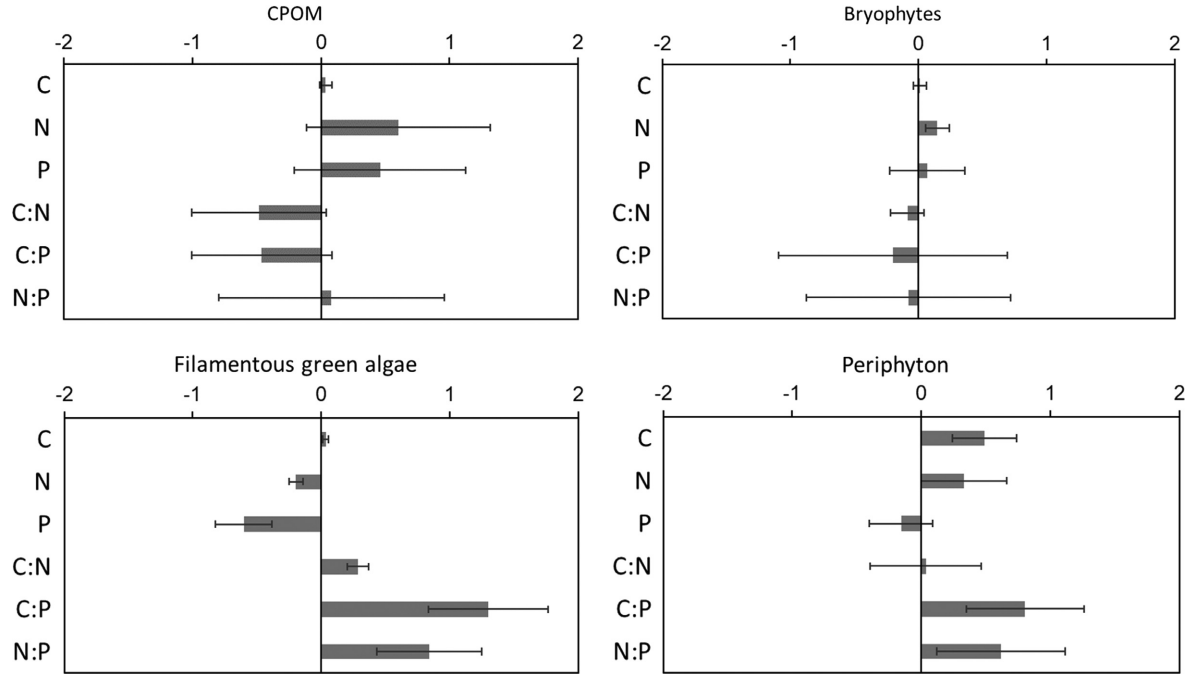

FIG. 5. Proportional changes in C, N, P (% w/w) and molar C:N:P stoichiometric ratios in the basal food web resources due to sucrose addition based on the before and after control impact experimental design. Error bars represent SE; CPOM, coarse particulate organic matter.

Effects of carbon additions

The small carbon addition had large effects on carbon fluxes and metabolic efficiencies (see Fig. 8, Appendix S1: Tables S7 and S8). While GPP increased slightly over the whole treatment period (12%), there was a small relative increase in light use efficiency (37%). ER intensified by 70%, and the net ecosystem production (NEP) became relatively more negative by 125%, i.e., 125% relative increase in biotic CO_2 emissions. Heterotrophic respiration and production increased by 89%, and this was reflected by a shorter (−40%) uptake length ($S_{w\text{-}OC}$) and faster mineralization velocity (92%) of organic carbon. The proportion of natural allochthonous DOC flux respired (range 2.2–5.3%) and organic carbon use efficiency by bacteria (range 0.1–0.3%) increased by 112% at the reach scale.

DISCUSSION

The use of a before and after control impact experiment together with the addition of a deliberate tracer with a distinctive $\delta^{13}C$ signature allowed not only to trace the fate of the added carbon into the treated reach but also to build the flow food web of the control reach, unravel C reciprocal subsidies between autotrophs and bacteria, and demonstrate the potential for some natural allochthonous organic matter to feed the primary producers via bacterial respiration. Our experiment showed that a small continuous addition of labile DOM (0.52 mg C/L as sucrose, 12% of total DOC, Appendix S1: Fig. S1) can profoundly alter whole-ecosystem behavior (see also Warren et al. 1964, Lutz et al. 2012, Robbins et al. 2017).

Reciprocal subsidies between autotrophs and bacteria

The use of bacterial CO_2 by autotrophs has long been part of lake, marine, and earth-scale carbon cycles (Hutchinson 1948, Redfield 1958, Kuznetsov 1968), but has been overlooked in streams. Here we show that bacterial CO_2 can also be important in turbulent headwater streams, accounting for 37% of the CO_2 fixed by autotrophs in the control reach. This is possible within the intricate matrix of the biofilm (e.g., Kamjunke et al. 2015, Battin et al. 2016) or an algal mat, as when the CO_2 is released in the water column it is very quickly degassed to the atmosphere (here 5–15 minutes; Demars 2019). This is supported by a preferential uptake of bacterial CO_2 in autotrophs relative to total flux of CO_2: 1.4 ± 1.1 and 1.7 ± 1.4 in the control and treatment reach, respectively (calculated as bacterial CO_2 relative to total CO_2 fixed by autotrophs compared to heterotrophic respiration relative to total CO_2 emissions).

The results suggest a significant proportion of autotrophic C ($19 \pm 9\%$) was derived from allochthonous DOM via bacterial respiration in the control (Fig. 6). The bacterial CO_2 flux to autotrophs assumed its $\delta^{13}C$ signature was the same as that of the bacteria (as in Collins et al. 2016), and the proportion of C sources the

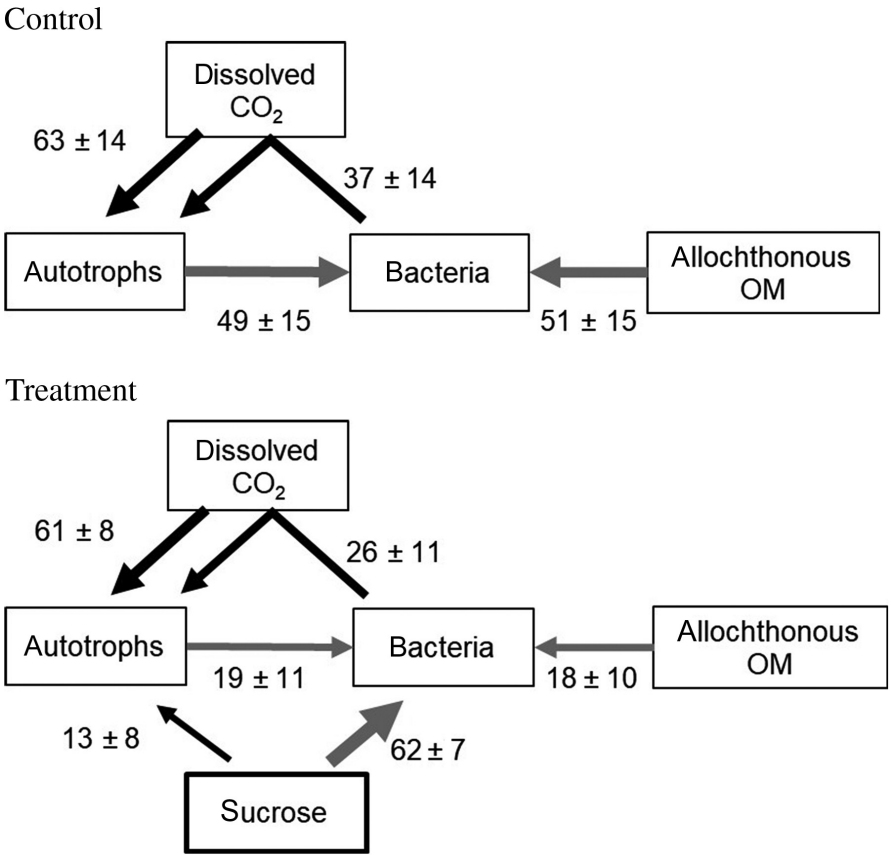

FIG. 6. Carbon source partitioning of autotrophs (black arrows) and bacteria (gray arrows) in the control (top) and treated reach (bottom) after three weeks of sucrose addition. Numbers represent the proportion (%) of the sources and their uncertainties (SD). The calculations were based on carbon stable isotope analyses ($\delta^{13}C$) and the fraction of sucrose in the different compartments (Appendix S1: Tables S3 and S4).

same as for bacterial production. The controlled experiment allowed us to calculate the bacterial respiration of the added sucrose as 2.16 g $C \cdot m^{-2} \cdot d^{-1}$ over the three weeks of sucrose addition. This represented 82% (53–184%) of the estimated treatment bacterial respiration (2.64 ± 1.45 g $C \cdot m^{-2} \cdot d^{-1}$, Appendix S1: Table S8) and the proportion of sucrose in bacteria was estimated at 62% ± 7% (Fig. 6). So the estimates were still within measurement errors. The proportion of DOM channeled to autotrophs via bacterial respiration was similar in the treatment (21% ± 8%), more from sucrose (16% ± 7%) than natural DOM (5% ± 3%). This microbial loop allows part of the allochthonous DOM processed by bacteria (brown web) to be incorporated into autotrophs (green web), likely increasing the quality of food available to consumers (Brett et al. 2017).

The use of autotrophic C by bacteria was reduced by the sucrose addition despite a small increase in GPP. Bacterial production in the treatment relied more on sucrose than autotrophs and natural allochthonous organic matter, assuming a similar bacterial growth efficiency for all sources (range 5–20%), which is plausible under nutrient limitations (del Giorgio and Cole 1998) and corresponded to previous studies (e.g., Berggren et al. 2009, Fasching et al. 2014, Berggren and del Giorgio 2015). Overall, sucrose addition shifted the reciprocal carbon exchange between bacteria and autotrophs to a predominantly one-way flow from bacteria to autotrophs.

Boom and bust: role of nutrients

Gross primary productivity (GPP) appeared to be stimulated by the addition of sucrose (contrary to expectations under nutrient limitations, Fig. 1) but this was short lived, despite sustained light availability during the addition period (Fig. 3). Heterotrophic respiration of sucrose (independent of NPP) peaked after two weeks but crashed within days while the supply of sucrose was continuously flowing through the reach (with sucrose concentration increasing from 0.22 to 0.88 mg C/L with falling discharge, Appendix S1: Fig. S4). This was in sharp contrast to the peaks in respiration followed by a more sustained response of ecosystem (mostly heterotrophic) respiration to hydrological connectivity with soil water in the control reaches (Fig. 3; see Demars

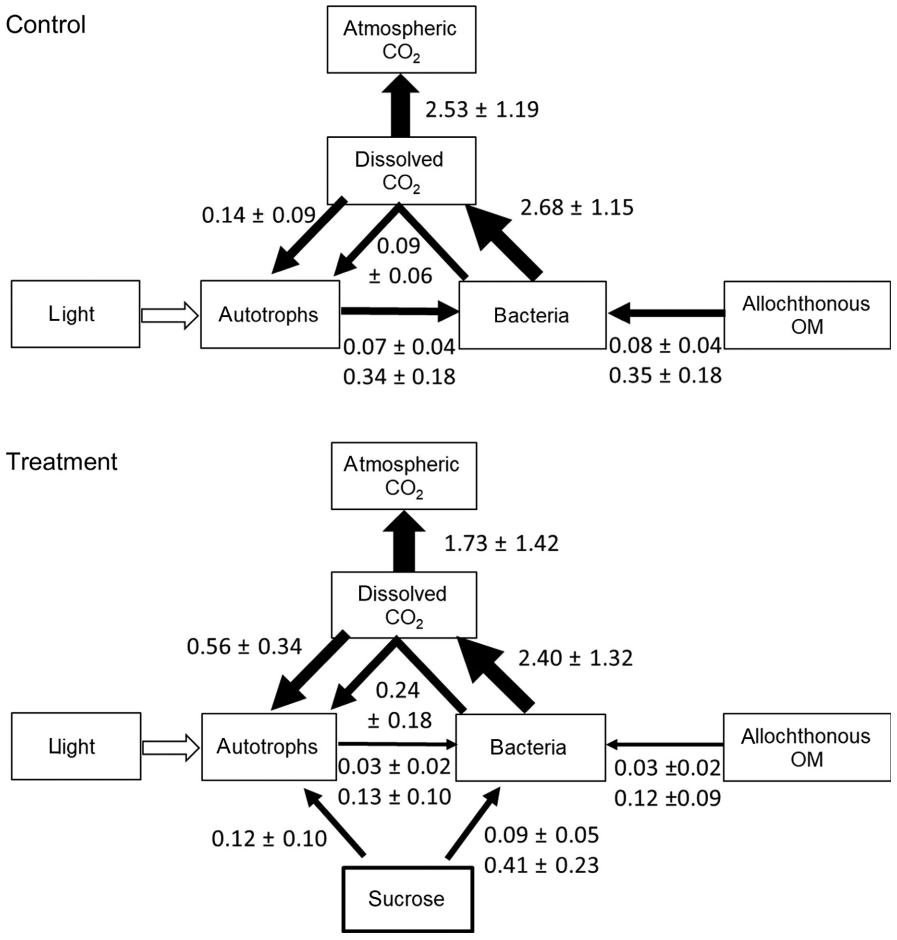

FIG. 7. Flow food webs and biotic CO_2 emissions under stable flows: in-stream biotic carbon fluxes (g $C \cdot m^{-2} \cdot d^{-1}$, black arrows) in the control (top) and treatment reach (bottom) after three weeks of sucrose addition, based on source partitioning using stable isotopes (end of experiment) and production estimates (average during sucrose addition). The C fluxes going to autotrophs and bacteria represent rates of biomass accrual, i.e., net primary production and heterotrophic production. Bacterial respiration and net ecosystem production (biotic CO_2 emissions) were similar in the control and the treatment (unlike expectations in Fig. 1) because the stream water of the control reach was hydrologically still connected to soils at the beginning of the treatment period (Fig. 3), unlike the treatment reach, which had negligible lateral inflows but see Fig. 8 for the effects. Two estimates were given for bacterial production based on heterotrophic growth efficiencies (HGE) of 0.05 (low) and 0.2 (moderate). The uncertainties represent SD (68% confidence interval, see Discussion, Uncertainties for interpretation of uncertainties in unreplicated studies).

2019). This boom and bust in the treatment reach was likely due to nutrient limitations for both autotrophs and eventually heterotrophs (e.g., Peterson et al. 1985, Kominoski et al. 2018), by both N and P according to the changes in filamentous green algae and periphyton C:N:P stoichiometry (C:N:P = 632:49:1 and 428:38:1, respectively), and relative to the optimal ratio for growth (C:N:P = 119:17:1 to 158:18:1; Kahlert 1998, Hillebrand and Sommer 1999).

The shortfall of nutrients (N, P) was not compensated by faster nutrient cycling rates, as observed in previous studies with much higher concentrations of labile DOM additions (e.g., Bernhardt and Likens 2002), possibly due to increased bacterial retention at ecosystem scale (Roberts and Mulholland 2007). This may also be due to limitation of phosphate uptake by NH_4 availability (long term median in both streams 7 μg N/L) in streams relatively rich in nitrate (see Oviedo-Vargas et al. 2013).

The observed pulse of ER due to sucrose addition seemed to mirror GPP with a 4-d time lag, but heterotrophic respiration was much larger and mostly independent of NPP (GPP and carbon use efficiency by autotrophs, Appendix S1: Fig. S5). So, while the small peak in GPP was neither predicted (under the assumption of nutrient limitation, Fig. 1) nor observed in the control reaches (Demars 2019), sucrose addition did shift the metabolic balance toward heterotrophy. The shift in heterotrophy was not so obvious in the comparative flow food webs (see Fig. 7), but differences in size effects with the more robust BACI design were clear: only +12% for GPP but +70% for ER and +89% for heterotrophic respiration (Fig. 8).

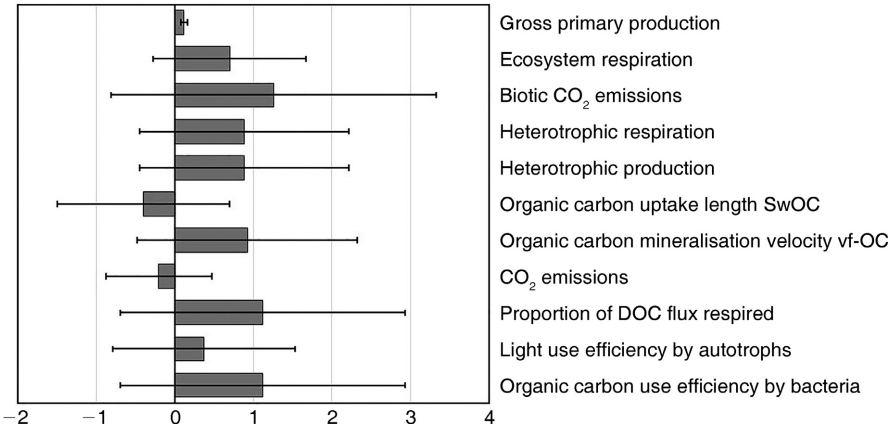

FIG. 8. Relative effect size of sucrose addition (change relative to the mean, 1 = 100%) on selected ecosystem properties at reach scale based on the before and after control impact experimental design. Error bars are ± SD (equivalent to 68% confidence interval), not the usual standard error of the mean because the study was unreplicated and without *P* values. Many of the responses from individual ecosystem properties followed expectations from previous studies, hence error bars could be considerably reduced by replicating the experiment (see Discussion, Uncertainties). See Appendix S1: Tables S7 and S8 for individual values.

A small increase in GPP following sucrose addition has been observed before under similar experimental conditions (Robbins et al. 2017). This transient response may be explained by the increase in supply of CO_2 by bacteria and an initial sufficiency of nutrients (N, P).

Fate of carbon

By and far, the largest quantity of carbon processed by bacteria was lost as CO_2 emission. Heterotrophic respiration over the treated reach respired (on average) 35% of the added sucrose. Bacterial production averaged 2–10% of the sucrose flux within the studied reach. Heterotrophic respiration of natural allochthonous DOM was about 3% in the control stream and 2.2% prior to sucrose addition in the treatment. The fact that sucrose was processed 10 times faster than natural stream DOM was well reflected by the shortening of the organic uptake length ($S_{w\text{-}OC}$) and increased mineralization velocity ($v_{f\text{-}OC}$). This was expected (see, e.g., Marcarelli et al. 2011, Mineau et al. 2016). However the average rates of mineralization of natural DOM at the soil–water interface in both streams (scaled up to the first-order catchment) were relatively high: 22% ± 10% (Birnie) and 31% ± 15% (Cairn) under stable flows, with peaks over 50% (Demars 2019). The changes in organic uptake lengths in the control and the differences between control and treatment prior to sucrose addition can be explained by the loss of hydrological connectivity with soil water, as indicated by the changes in soil moisture, and the difference in lateral inflows between the control (10.7%) and the treatment (2.3%). The shortening of the organic uptake length ($S_{w\text{-}OC}$) reflected more hydrological changes as indicated by the different direction of change in organic carbon uptake ($v_{f\text{-}OC}$) between the control and the treatment. In the control $v_{f\text{-}OC}$ declined by 32% against a 52% decline in DOM supply. In contrast, $v_{f\text{-}OC}$ increased by 43% in the treatment with the addition of labile carbon, despite a 55% fall in DOM supply (similar to the control). Overall, the uptake lengths of natural DOM (i.e., excluding those influenced by sucrose addition) were longer (2.5–4.3 km) than the length of the first-order streams studied here (1 km), and so a large part of the carbon is released to downstream ecosystems as previously observed (e.g., Wiegner et al. 2005), especially during times of loss of hydrological connectivity with the soil of the catchment (Demars 2019).

The treatment reach did not show the large peaks in respiration (outside the period of sucrose addition) that the control reaches showed when the catchment was hydrologically connected, as indicated by soil moisture (Fig. 3; Demars 2019). This is likely because the treatment reach is a more constrained reach largely disconnected from the land. It was initially chosen to avoid lateral inflows, which were very small (2.3%) and mostly from a spring fed flush (i.e., groundwater), rather than seepage from organic and riparian soils known to stimulate bacterial activity (e.g., Brunke and Gonser 1997, Pusch et al. 1998). Interestingly, the average bacterial respiration was similar in the control and treatment reaches over the three weeks of sucrose addition (Fig. 7), suggesting part of the organic matter respired in the control was relatively labile and comparable to the 0.5 mg C/L of added sucrose. The dynamic of this respiration within the three weeks was very different however, decreasing with the progressive loss of hydrological connectivity with soils in the control, and peaking after two weeks in the treatment (Fig. 3), also independently of GPP (Appendix S1: Fig S5).

Sucrose is very labile and is well known to promote the growth of filamentous bacteria *Sphaerotilus natans* ("sewage fungus"), even at relatively low concentrations (0.25–1.00 mg/L) in a stable flow forested stream

(Warren et al. 1964). This was not observed in this study, likely because the moorland streams studied here were more open and colonized by *Microspora*, a common genus of filamentous green algae in Scottish streams (Kinross et al. 1993). *Microspora* was likely able to uptake sucrose by osmotrophy (Wright and Hobbie 1966) but this accounted for only 13% of C uptake by *Microspora*. Overall daily uptake of sucrose by autotrophs represented 1.6% of the average daily flux of sucrose.

Uncertainties

We strived to quantify and propagate uncertainties in all our calculations. These uncertainties may appear large, particularly for the effect size of ecosystem properties presented in Fig. 8. It was clear from the discussion that previous studies produced similar results for individual effects, and thus error bars could be considerably reduced by replicating this experiment allowing the calculation of a standard error (SE) and statistical significance (P value). Since $SE = \delta x/\sqrt{n}$ with δx standard deviation and n the number of replicates, just four replicates could potentially divide the error bars by two and make 80% of the effects presented in Fig. 8 significant (assuming independent experiments produced the same results).

Much of the C flux uncertainties in the flow food webs (Fig. 7) did not come from C source partitioning (see Fig. 6), but rather from the estimation of net autotrophic and net heterotrophic ecosystem production (Appendix S1: Table S8). The estimation of net autotrophic production will likely remain challenging (e.g., Demars et al. 2015) but bacterial growth efficiency should be determined in future studies.

The autotrophs did not include bryophytes in our flow food web calculations because their contribution to primary production was thought to be negligible over the few weeks of the experiment, and particularly toward the end of the experiment when filamentous green algae were covering bryophytes. The lack of bryophyte growth under very low phosphorus concentrations (here 2–4 μg P/L of soluble reactive P) combined with shading by epiphytes has been well documented (e.g., Finlay and Bowden 1994). This may also explain the lack of changes in bryophyte C:N:P stoichiometry (Fig. 5).

Conclusions

Part of the carbon derived from allochthonous organic matter can feed the autotrophs via the CO_2 produced by stream bacterial respiration, intermingling the green and brown webs. The preferential uptake of labile carbon (sucrose) by bacteria and excess bacterial CO_2 relative to nutrients (N, P) for autotrophs shifted the reciprocal carbon exchange between bacteria and autotrophs to a predominantly one-way carbon flow from bacteria to autotrophs. Light use efficiency by autotrophs increased, but so did the C:N:P molar ratios of autotrophs, the latter likely to become less palatable to consumers. The bacterial response to sucrose addition shifted the metabolic balance toward heterotrophy, increasing organic carbon use efficiency and biotic CO_2 emissions, shortening carbon uptake length (average distance travelled by a molecule of organic matter) and providing less organic matter of lower quality for downstream ecosystems.

Even a small increase in labile dissolved organic matter supply due to climate and land use change could alter instream carbon cycling, with large effects on stream food web and biogeochemistry in small streams draining catchments with soils rich in organic carbon. These effects could be accrued by climate change, notably temperature increase, thawing of permafrost and rainfall increase in boreal ecosystems with soils rich in organic matter.

Acknowledgments

We thank Carol Taylor and Helen Watson for managing the long-term monitoring, Yvonne Cook and Susan McIntyre for running water chemical analyses, Claire Abel for the phospholipid fatty acid extraction, Maureen Procee for running the compound specific isotope ratio analysis, Gillian Martin for preparing and running the samples for stable isotope ratio analysis, Glensaugh farm manager Donald Barrie for hosting BOLD during the experiment and facilitating the work, Baptiste Marteau and two anonymous referees for comments on the manuscript. This study was funded by the Scottish Government Rural and Environmental Science and Analytical Services (RESAS), with additional funding support as part of the UK Environmental Change Network (ECN), and NERC Macronutrient Cycles Program. The writing up was partly funded by the Norwegian institute for water research (NIVA). The authors acknowledge the provision of data forming part of the ECN-wide data set, https://catalogue.ceh.ac.uk/documents/456c24dd-0fe8-46c0-8ba5-855c001bc05f

Literature Cited

Amin, S. A., et al. 2015. Interaction and signalling between a cosmopolitan phytoplankton and associated bacteria. Nature 522:98–101.

Augspurger, C., G. Gleixner, C. Kramer, and K. Kusel. 2008. Tracking carbon flow in a 2-week-old and 6-week-old stream biofilm food web. Limnology and Oceanography 53:642–650.

Battin, T. J., K. Besemer, M. M. Bengtsson, A. M. Romani, and A. I. Packmann. 2016. The ecology and biogeochemistry of stream biofilms. Nature Reviews Microbiology 14:251–263.

Beaulieu, J. J., C. P. Arango, D. A. Balz, and W. D. Shuster. 2013. Continuous monitoring reveals multiple controls on ecosystem metabolism in a suburban stream. Freshwater Biology 58:918–937.

Bec, A., M.-E. Perga, A. Koussoroplis, G. Bardoux, C. Desvilettes, G. Bourdier, and A. Mariotti. 2011. Assessing the reliability of fatty acid-specific stable isotope analysis for trophic studies. Methods in Ecology and Evolution 2:651–659.

Berggren, M., and P. A. del Giorgio. 2015. Distinct patterns of microbial metabolism associated to riverine dissolved organic carbon of different source and quality. Journal of Geophysical Research—Biogeosciences 120:989–999.

Berggren, M., H. Laudon, and M. Jansson. 2009. Hydrological control of organic carbon support for bacterial growth in boreal headwater streams. Microbial Ecology 57:170–178.

Berggren, M., J. F. Lapierre, and P. A. del Giorgio. 2012. Magnitude and regulation of bacterioplankton respiratory quotient across freshwater environmental gradients. Isme Journal 6:984–993.

Bernhardt, E. S., and G. E. Likens. 2002. Dissolved organic carbon enrichment alters nitrogen dynamics in a forest stream. Ecology 83:1689–1700.

Bernhardt, E. S., et al. 2018. The metabolic regimes of flowing waters. Limnology and Oceanography 63:S99–S118.

Bligh, E. G., and W. J. Dyer. 1959. A rapid method of total lipid extraction and purification. Canadian Journal of Biochemistry and Physiology 37:911–917.

Boller, A., P. Thomas, C. Cavanaugh, and K. Scott. 2015. Isotopic discrimination and kinetic parameters of RubisCO from the marine bloom-forming diatom, *Skeletonema costatum*. Geobiology 13:33–43.

Boschker, H. T. S., and J. J. Middelburg. 2002. Stable isotopes and biomarkers in microbial ecology. Fems Microbiology Ecology 40:85–95.

Boye, K., V. Noel, M. M. Tfaily, S. E. Bone, K. H. Williams, J. R. Bargar, and S. Fendorf. 2017. Thermodynamically controlled preservation of organic carbon in floodplains. Nature Geoscience 10:415–419.

Brett, M. T. 2014. Resource polygon geometry predicts Bayesian stable isotope mixing model bias. Marine Ecology Progress Series 514:1–12.

Brett, M. T., et al. 2017. How important are terrestrial organic carbon inputs for secondary production in freshwater ecosystems? Freshwater Biology 62:833–853.

Brunke, M., and T. Gonser. 1997. The ecological significance of exchange processes between rivers and groundwater. Freshwater Biology 37:1–33.

Butenschoen, M., et al. 2016. ERSEM 15.06: a generic model for marine biogeochemistry and the ecosystem dynamics of the lower trophic levels. Geoscientific Model Development 9:1293–1339.

Butler, J. N. 1982. Carbon dioxide equilibria and their applications. First edition. Addison-Wesley, Reading, UK.

Carroll, J. J., J. D. Slupsky, and A. E. Mather. 1991. The solubility of carbon dioxide in water at low pressure. Journal of Physical and Chemical Reference Data 20:1201–1209.

Certini, G., C. D. Campbell, and A. C. Edwards. 2004. Rock fragments in soil support a different microbial community from the fine earth. Soil Biology and Biochemistry 36:1119–1128.

Cole, J. J. 2013. Freshwater ecosystems and the carbon cycle. International Ecology Institute, Oldendorf, Germany.

Collins, S. M., J. P. Sparks, S. A. Thomas, S. A. Wheatley, and A. S. Flecker. 2016. Increased light availability reduces the importance of bacterial carbon in headwater stream food webs. Ecosystems 19:396–410.

Cooper, R., V. Thoss, and H. Watson. 2007. Factors influencing the release of dissolved organic carbon and dissolved forms of nitrogen from a small upland headwater during autumn runoff events. Hydrological Processes 21:622–633.

Cotner, J. B., E. K. Hall, J. T. Scott, and M. Heldal. 2010. Freshwater bacteria are stoichiometrically flexible with a nutrient composition similar to seston. Frontiers in Microbiology 1:132.

Cummins, K. W., J. J. Klug, R. G. Wetzel, R. C. Petersen, K. F. Suberkropp, B. A. Manny, J. C. Wuycheck, and F. O. Howard. 1972. Organic enrichment with leaf leachate in experimental lotic ecosystems. BioScience 22:719–722.

Davidson, J. F., and E. J. Cullen. 1957. The determination of diffusion coefficients for sparingly solubles gases in liquids. Transactions of the Institution of Chemical Engineers (Great Britain) 35:51–60.

Dawson, J. J. C. 2013. Losses of soil carbon to the atmosphere via inland surface waters. Pages 183–208 *in* R. Lal, editor. Ecosystem services and carbon sequestration in the biosphere. Springer Science, Dordrecht, The Netherlands.

de Castro, D. M. P., D. R. de Carvalho, P. D. Pompeu, M. Z. Moreira, G. B. Nardoto, and M. Callisto. 2016. Land use influences niche size and the assimilation of resources by benthic macroinvertebrates in tropical headwater streams. PLoS ONE 11:e0150527.

del Giorgio, P. A., and J. J. Cole. 1998. Bacterial growth efficiency in natural aquatic systems. Annual Review of Ecology and Systematics 29:503–541.

Demars, B. O. L. 2008. Whole-stream phosphorus cycling: testing methods to assess the effect of saturation of sorption capacity on nutrient uptake length measurements. Water Research 42:2507–2516.

Demars, B. O. L. 2019. Hydrological pulses and burning of dissolved organic carbon by stream respiration. Limnology and Oceanography 64:406–421.

Demars, B. O. L., and A. C. Edwards. 2007. Tissue nutrient concentrations in freshwater aquatic macrophytes: high intertaxon differences and low phenotypic response to nutrient supply. Freshwater Biology 52:2073–2086.

Demars, B. O. L., J. R. Manson, J. S. Olafsson, G. M. Gislason, R. Gudmundsdottir, G. Woodward, J. Reiss, D. E. Pichler, J. J. Rasmussen, and N. Friberg. 2011. Temperature and the metabolic balance of streams. Freshwater Biology 56:1106–1121.

Demars, B. O. L., J. Thompson, and J. R. Manson. 2015. Stream metabolism and the open diel oxygen method: principles, practice, and perspectives. Limnology and Oceanography—Methods 13:356–374.

Demars, B. O. L., G. M. Gislason, J. S. Olafsson, J. R. Manson, N. Friberg, J. M. Hood, J. J. D. Thompson, and T. E. Freitag. 2016. Impact of warming on CO_2 emissions from streams countered by aquatic photosynthesis. Nature Geoscience 9:758–761.

Demars, B. O. L., J. Thompson, and J. R. Manson. 2017. Stream metabolism and the open diel oxygen method: principles, practice, and perspectives (vol 13, pg 356, 2015). Limnology and Oceanography-Methods 15:219.

Drake, T. W., K. P. Wickland, R. G. M. Spencer, D. M. McKnight, and R. G. Striegl. 2015. Ancient low-molecular-weight organic acids in permafrost fuel rapid carbon dioxide production upon thaw. Proceedings of the National Academy of Sciences USA 112:13946–13951.

Drake, T. W., P. A. Raymond, and R. G. M. Spencer. 2018. Terrestrial carbon inputs to inland waters: a current synthesis of estimates and uncertainty. Limnology and Oceanography Letters 3:132–142.

Dungait, J. A. J., D. W. Hopkins, A. S. Gregory, and A. P. Whitmore. 2012. Soil organic matter turnover is governed by accessibility not recalcitrance. Global Change Biology 18:1781–1796.

Evans, C. D., M. N. Futter, F. Moldan, S. Valinia, Z. Frogbrook, and D. N. Kothawala. 2017. Variability in organic carbon reactivity across lake residence time and trophic gradients. Nature Geoscience 10:832–835.

Fasching, C., B. Behounek, G. A. Singer, and T. J. Battin. 2014. Microbial degradation of terrigenous dissolved organic matter and potential consequences for carbon cycling in brownwater streams. Scientific Reports 4:4981.

Finlay, J. C., and W. B. Bowden. 1994. Controls on production of bryophytes in an Arctic tundra stream. Freshwater Biology 32:455–465.

Freeman, C., N. Fenner, N. J. Ostle, H. Kang, D. J. Dowrick, B. Reynolds, M. A. Lock, D. Sleep, S. Hughes, and J. Hudson. 2004. Export of dissolved organic carbon from peatlands under elevated carbon dioxide levels. Nature 430:195–198.

Friberg, N., and M. J. Winterbourn. 1996. Interactions between riparian leaves and algal/microbial activity in streams. Hydrobiologia 341:51–56.

Frostegård, A., A. Tunlid, and E. Baath. 1993. Phospholipid fatty acid composition, biomass, and activity of microbial communities from two soil types experimentally exposed to different heavy metals. Applied and Environmental Microbiology 59:3605–3617.

Gladyshev, M. I., N. N. Sushchik, O. V. Anishchenko, O. N. Makhutova, V. I. Kolmakov, G. S. Kalachova, A. A. Kolmakova, and O. P. Dubovskaya. 2011. Efficiency of transfer of essential polyunsaturated fatty acids versus organic carbon from producers to consumers in a eutrophic reservoir. Oecologia 165:521–531.

Grossart, H. P. 2010. Ecological consequences of bacterioplankton lifestyles: changes in concepts are needed. Environmental Microbiology Reports 2:706–714.

Hall, R. O. 1995. Use of a stable carbon isotope addition to trace bacterial carbon through a stream food web. Journal of the North American Benthological Society 14:269–277.

Hall, R. O., and H. L. Madinger. 2018. Use of argon to measure gas exchange in turbulent mountain streams. Biogeosciences 15:3085–3092.

Hall, R. O., and J. L. Meyer. 1998. The trophic significance of bacteria in a detritus-based stream food web. Ecology 79:1995–2012.

Hall, R. O. Jr., J. L. Tank, M. A. Baker, E. J. Rosi-Marshall, and E. R. Hotchkiss. 2016. Metabolism, gas exchange, and carbon spiraling in rivers. Ecosystems 19:73–86.

Hartley, A. M., W. A. House, B. S. C. Leadbeater, and M. E. Callow. 1996. The use of microelectrodes to study the precipitation of calcite upon algal biofilms. Journal of Colloid and Interface Science 183:498–505.

Hasler, C. T., D. Butman, J. D. Jeffrey, and C. D. Suski. 2016. Freshwater biota and rising pCO_2? Ecology Letters 19:98–108.

Hayes, J. M. 2001. Fractionation of the isotopes of carbon and hydrogen in biosynthetic processes. Pages 225–277 *in* J. W. Valley, and D. Cole, editors. Stable isotope geochemistry. Mineralogical Society of America, Boston, Massachusetts, USA.

Hessen, D. O., G. I. Ågren, T. R. Anderson, J. J. Elser, and P. C. De Ruiter. 2004. Carbon sequestration in ecosystems: the role of stoichiometry. Ecology 85:1179–1192.

Hill Farming Research Organisation. 1983. Glensaugh Research Station. D & J Croal, Haddington, UK.

Hillebrand, H., and U. Sommer. 1999. The nutrient stoichiometry of benthic microalgal growth: redfield proportions are optimal. Limnology and Oceanography 44:440–446.

Hotchkiss, E. R., and R. O. Hall. 2015. Whole-stream C-13 tracer addition reveals distinct fates of newly fixed carbon. Ecology 96:403–416.

Hurlbert, S. H. 1984. Pseudoreplication and the design of ecological field experiments. Ecological Monographs 54:187–211.

Huryn, A. D., J. P. Benstead, and S. M. Parker. 2014. Seasonal changes in light availability modify the temperature dependence of ecosystem metabolism in an arctic stream. Ecology 95:2826–2839.

Hutchinson, G. E. 1948. Circular causal systems in ecology. Annals: New York Academy of Sciences 50:221–246.

Jahren, A. H., C. Saudek, E. H. Yeung, W. H. L. Kao, R. A. Kraft, and B. Caballero. 2006. An isotopic method for quantifying sweeteners derived from corn and sugar cane. American Journal of Clinical Nutrition 84:1380–1384.

Kahlert, M. 1998. C:N: P ratios of freshwater benthic algae. Archiv für Hydrobiologie, Advances in Limnology 51:105–114.

Kamjunke, N., P. Herzsprung, and T. R. Neu. 2015. Quality of dissolved organic matter affects planktonic but not biofilm bacterial production in streams. Science of the Total Environment 506:353–360.

Kankaala, P., S. Peura, H. Nykanen, E. Sonninen, S. Taipale, M. Tiirola, and R. I. Jones. 2010. Impacts of added dissolved organic carbon on boreal freshwater pelagic metabolism and food webs in mesocosm experiments. Fundamental and Applied Limnology 177:161–176.

Kinross, J. H., N. Christofi, P. A. Read, and R. Harriman. 1993. Filamentous algal communities related to pH in streams in The Trossachs, Scotland. Freshwater Biology 30:301–317.

Kominoski, J. S., A. D. Rosemond, J. P. Benstead, V. Gulis, and D. W. P. Manning. 2018. Experimental nitrogen and phosphorus additions increase rates of stream ecosystem respiration and carbon loss. Limnology and Oceanography 63:22–36.

Kuehn, K. A., S. N. Francoeur, R. H. Findlay, and R. K. Neely. 2014. Priming in the microbial landscape: periphytic algal stimulation of litter-associated microbial decomposers. Ecology 95:749–762.

Kuznetsov, S. I. 1968. Recent studies on the role of macroorganisms in cycling of substances in lakes. Limnology and Oceanography 13:211–224.

Lutz, B. D., E. S. Bernhardt, B. J. Roberts, R. M. Cory, and P. J. Mulholland. 2012. Distinguishing dynamics of dissolved organic matter components in a forested stream using kinetic enrichments. Limnology and Oceanography 57:76–89.

Lyon, D. R., and S. E. Ziegler. 2009. Carbon cycling within epilithic biofilm communities across a nutrient gradient of headwater streams. Limnology and Oceanography 54:439–449.

Main, C., H. Ruhl, D. Jones, A. Yool, B. Thornton, and D. Mayor. 2015. Hydrocarbon contamination affects deep-sea benthic oxygen uptake and microbial community composition. Deep Sea Research Part I: Oceanographic Research Papers 100:79–87.

Marcarelli, A. M., C. V. Baxter, M. M. Mineau, and R. O. Jr Hall. 2011. Quantity and quality: unifying food web and ecosystem perspectives on the role of resource subsidies in freshwaters. Ecology 92:1215–1225.

Marin-Spiotta, E., K. E. Gruley, J. Crawford, E. E. Atkinson, J. R. Miesel, S. Greene, C. Cardona-Correa, and R. G. M. Spencer. 2014. Paradigm shifts in soil organic matter research affect interpretations of aquatic carbon cycling: transcending disciplinary and ecosystem boundaries. Biogeochemistry 117:279–297.

McNevin, D. B., M. R. Badger, S. M. Whitney, S. von Caemmerer, G. G. Tcherkez, and G. D. Farquhar. 2007. Differences in carbon isotope discrimination of three variants of d-ribulose-1, 5-bisphosphate carboxylase/oxygenase reflect differences in their catalytic mechanisms. Journal of Biological Chemistry 282:36068–36076.

Mineau, M. M., W. M. Wollheim, I. Buffam, S. E. G. Findlay, R. O. Hall, E. R. Hotchkiss, L. E. Koenig, W. H. McDowell, and T. B. Parr. 2016. Dissolved organic carbon uptake in streams: a review and assessment of reach-scale measurements. Journal of Geophysical Research—Biogeosciences 121:2019–2029.

Monteith, D. T., et al. 2007. Dissolved organic carbon trends resulting from changes in atmospheric deposition chemistry. Nature 450:537–539.

Morel, A., and R. C. Smith. 1974. Relation between total quanta and total energy for aquatic photosynthesis. Limnology and Oceanography 19:591–600.

Mulholland, P. J., et al. 2002. Can uptake length in streams be determined by nutrient addition experiments? Results from an interbiome comparison study. Journal of the North American Benthological Society 21:544–560.

Muller-Navarra, D. C., M. T. Brett, A. M. Liston, and C. R. Goldman. 2000. A highly unsaturated fatty acid predicts carbon transfer between primary producers and consumers. Nature 403:74–77.

Neal, C., W. A. House, and K. Down. 1998. An assessment of excess carbon dioxide partial pressures in natural waters based on pH and alkalinity measurements. Science of the Total Environment 210/211:173–185.

Neely, R. K., and R. G. Wetzel. 1995. Simultaneous use of 14C and 3H to determine autotrophic production and bacterial protein production in periphyton. Microbial Ecology 30:227–237.

Newbold, J. D., P. J. Mulholland, J. W. Elwood, and R. V. Oneill. 1982. Organic carbon spiralling in stream ecosystems. Oikos 38:266–272.

Odum, H. T. 1956. Primary production in flowing waters. Limnology and Oceanography 1:102–117.

Oviedo-Vargas, D., T. V. Royer, and L. T. Johnson. 2013. Dissolved organic carbon manipulation reveals coupled cycling of carbon, nitrogen, and phosphorus in a nitrogen-rich stream. Limnology and Oceanography 58:1196–1206.

Palmer, S. M., D. Hope, M. F. Billett, F. H. Dawson, and C. L. Bryant. 2001. Sources of organic and inorganic carbon in a headwater stream: evidence form carbon isotope studies. Biogeochemistry 52:321–338.

Parkyn, S. M., J. M. Quinn, T. J. Cox, and N. Broekhuizen. 2005. Pathways of N and C uptake and transfer in stream food webs: an isotope enrichment experiment. Journal of the North American Benthological Society 24:955–975.

Parnell, A. C., R. Inger, S. Bearhop, and A. L. Jackson. 2010. Source partitioning using stable isotopes: coping with too much variation. PLoS ONE 5:e9672.

Parnell, A. C., D. L. Phillips, S. Bearhop, B. X. Semmens, E. J. Ward, J. W. Moore, A. L. Jackson, J. Grey, D. J. Kelly, and R. Inger. 2013. Bayesian stable isotope mixing models. Environmetrics 24:387–399.

Peterson, B. J., et al. 1985. Transformation of a tundra river from heterotrophy to autotrophy by addition of phosphorus. Science 229:1383–1386.

Phillips, D. L., and J. W. Gregg. 2001. Uncertainty in source partitioning using stable isotopes. Oecologia 127:171–179.

Pusch, M., D. Fiebig, I. Brettar, H. Eisenmann, B. K. Ellis, L. A. Kaplan, M. A. Lock, M. W. Naegeli, and W. Traunspurger. 1998. The role of micro-organisms in the ecological connectivity of running waters. Freshwater Biology 40:453–495.

R Core Team. 2018. R: A language and environment for statistical computing. R Foundation for Statistical Computing, Vienna, Austria.www.R-project.org.

Raven, J. A., A. M. Johnston, J. R. Newman, and C. M. Scrimgeour. 1994. Inorganic carbon acquisition by aquatic photolithotrophs of the Dighty Burn, Angus, UK—Uses and limitations of natural abundance measurements of carbon isotopes. New Phytologist 127:271–286.

Redfield, A. C. 1958. The biological control of chemical factors in the environment. American Scientist 46:205–221.

Risse-Buhl, U., N. Trefzger, A. G. Seifert, W. Schonborn, G. Gleixner, and K. Kusel. 2012. Tracking the autochthonous carbon transfer in stream biofilm food webs. Fems Microbiology Ecology 79:118–131.

Robbins, C. J., R. S. King, A. D. Yeager, C. M. Walker, J. A. Back, R. D. Doyle, and D. F. Whigham. 2017. Low-level addition of dissolved organic carbon increases basal ecosystem function in a boreal headwater stream. Ecosphere 8: e01739.

Roberts, B. J., and P. J. Mulholland. 2007. In-stream biotic control on nutrient biogeochemistry in a forested stream, West Fork of Walker Branch. Journal of Geophysical Research—Biogeosciences 112:G04002.

Roberts, B. J., P. J. Mulholland, and W. R. Hill. 2007. Multiple scales of temporal variability in ecosystem metabolism rates: results from 2 years of continuous monitoring in a forested headwater stream. Ecosystems 10:588–606.

Schade, J. D., K. MacNeill, S. A. Thomas, F. C. McNeely, J. R. Welter, J. Hood, M. Goodrich, M. E. Power, and J. C. Finlay. 2011. The stoichiometry of nitrogen and phosphorus spiralling in heterotrophic and autotrophic streams. Freshwater Biology 56:424–436.

Schmidt, M. W. I., et al. 2011. Persistence of soil organic matter as an ecosystem property. Nature 478:49–56.

Southgate, D. A. T., and J. V. G. A. Durnin. 1970. Calorie conversion factors - an experimental reassessment of factors used in calculation of energy value of human diets. British Journal of Nutrition 24:517–535.

Stock, B. C., and B. X. Semmens. 2016. MixSIAR GUI User Manual. Version 3.1. https://github.com/brianstock/MixSIAR/, https://doi.org/10.5281/zenodo.47719

Stream Solute Workshop. 1990. Concepts and methods for assessing solute dynamics in stream ecosystems. Journal of the North American Benthological Society 9:95–119.

Stumm, W., and J. J. Morgan. 1981. Aquatic chemistry. An introduction emphasizing chemical equilibria in natural waters. Wiley Interscience, New York, New York, USA.

Stutter, M. I., D. G. Lumsdon, and A. P. Rowland. 2011. Three representative UK moorland soils show differences in decadal release of dissolved organic carbon in response to environmental change. Biogeosciences 8:3661–3675.

Stutter, M. I., S. M. Dunn, and D. G. Lumsdon. 2012. Dissolved organic carbon dynamics in a UK podzolic moorland catchment: linking storm hydrochemistry, flow path analysis and sorption experiments. Biogeosciences 9:2159–2175.

Stutter, M. I., S. Richards, and J. J. C. Dawson. 2013. Biodegradability of natural dissolved organic matter collected from a UK moorland stream. Water Research 47:1169–1180.

Taipale, S. J., E. Peltomaa, M. Hiltunen, R. I. Jones, M. W. Hahn, C. Biasi, and M. T. Brett. 2015. Inferring phytoplankton, terrestrial plant and bacteria bulk delta C-13 values from compound specific analyses of lipids and fatty acids. PLoS ONE 10:e0133974.

Tanentzap, A. J., et al. 2017. Terrestrial support of lake food webs: synthesis reveals controls over cross-ecosystem resource use. Science Advances 3:e1601765.

Uehlinger, U. 2006. Annual cycle and inter-annual variability of gross primary production and ecosystem respiration in a floodprone river during a 15-year period. Freshwater Biology 51:938–950.

Ulseth, A. J., E. Bertuzzo, G. A. Singer, J. Schelker, and T. J. Battin. 2018. Climate-induced changes in spring snowmelt impact ecosystem metabolism and carbon fluxes in an alpine stream network. Ecosystems 21:373–390.

Waldron, S., E. M. Scott, and C. Soulsby. 2007. Stable isotope analysis reveals lower-order river dissolved inorganic carbon pools are highly dynamic. Environmental Science & Technology 41:6156–6162.

Warren, D. E., J. H. Wales, G. E. Davis, and P. Doudoroff. 1964. Trout production in an experimental stream enriched with sucrose. Journal of Wildlife Management 28:617–660.

Wiegner, T. N., L. A. Kaplan, J. D. Newbold, and P. H. Ostrom. 2005. Contribution of dissolved organic C to stream metabolism: a mesocosm study using C-13-enriched tree-tissue leachate. Journal of the North American Benthological Society 24:48–67.

Wiegner, T. N., L. A. Kaplan, S. E. Ziegler, and R. H. Findlay. 2015. Consumption of terrestrial dissolved organic carbon by stream microorganisms. Aquatic Microbial Ecology 75:225–237.

Wilcox, H. S., J. B. Wallace, J. L. Meyer, and J. P. Benstead. 2005. Effects of labile carbon addition on a headwater stream food web. Limnology and Oceanography 50:1300–1312.

Williams, P. J. l. B., and P. A. del Giorgio. 2005. Respiration in aquatic ecosystems: history and background. Pages 1–17 *in* P. A. del Giorgio and P. J. l. B. Williams, editors. Respiration in aquatic ecosystems. Oxford University Press, Oxford, UK.

Wilson, H. F., J. E. Saiers, P. A. Raymond, and W. V. Sobczak. 2013. Hydrologic drivers and seasonality of dissolved organic carbon concentration, nitrogen content, bioavailability, and export in a forested New England stream. Ecosystems 16:604–616.

Wright, R. T., and J. E. Hobbie. 1966. Use of glucose and acetate by bacteria and algae in aquatic ecosystems. Ecology 47:447–464.

Young, R. G., and A. D. Huryn. 1998. Comment: improvements to the diurnal upstream-downstream dissolved oxygen change technique for determining whole-stream metabolism in small streams. Canadian Journal of Fisheries and Aquatic Sciences 55:1784–1785.

Supporting Information

Additional supporting information may be found online at: http://onlinelibrary.wiley.com/doi/10.1002/ecm.1399/full

Data Availability

Data are available on PANGAEA: https://doi.pangaea.de/10.1594/PANGAEA.909277